Exploring the Axiverse by Gravitational Waves and Gamma Rays

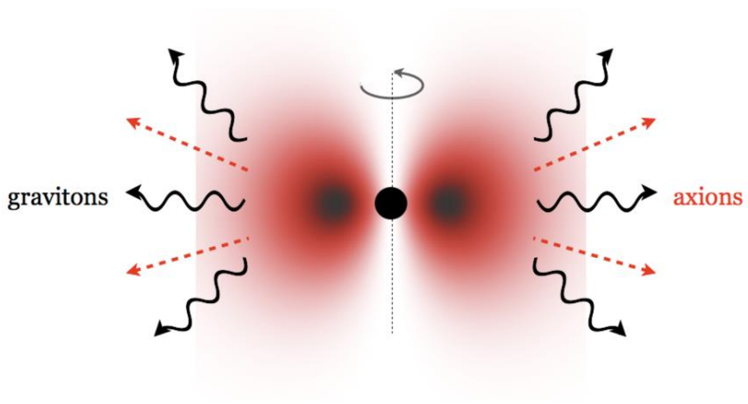

Hideo Kodama (KEK)

In collaboration with Hirotaka Yoshino, Kazunori Kohri and Kunihito Ioka

- H Yoshino, HK: PTP128, 153 (2012) [arXiv:1203.5070]
- ibid: PTEP2014, 043E02 (2014) [arXiv:1312.2326]
- K Kohiri, K Ioka, HK: in preparation

Cosmology Workshop 2014 @ IAS HKUST
(26 May 2014)

Find phenomena characteristic to string theory!!

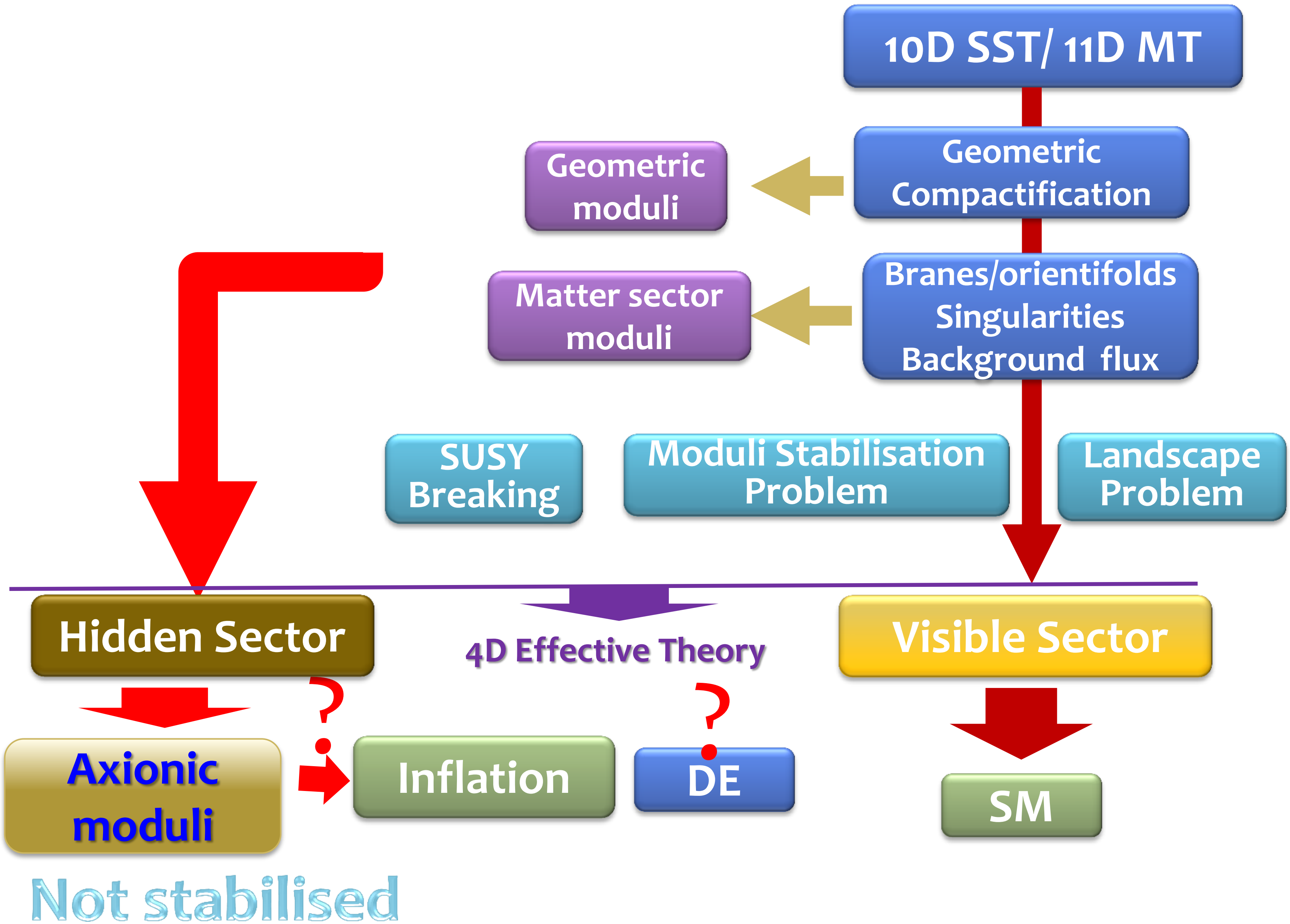

Axion Cosmophysics

Super-light axionic fields produce a rich vareity of new cosmophysical phenomena !!

Phenomena irrelevant to abundance

- Instabilities of black hole systems
- Influence on high-energy gamma ray propagation
- Solar activity/heat transport
- ……

Phenomena sensitive to abundance

- Deformation of the cosmological power spectrum
- Rotation of the CMB polarisation
- Dark matter/ Dark radiations
- Dark energy
- ……

Characteristic Mass Scales

- Compton wavelength= Horizon size (m=3H)
  - Present $t=t_0$: $m_0=4.5\times 10^{-33}$ eV
  - CMB last scattering $t=t_{ls}$: $m_{ls}=0.7\times 10^{-28}$ eV
  - H recombination $t=t_{rec}$: $m_{rec}=1.2\times 10^{-28}$ eV
  - Equidensity time $t=t_{eq}$: $m_{eq}=0.9\times 10^{-27}$ eV
- Compton wavelength= BH size ($1/m=M_{pl}^2/M$)
  - Supermassive BH $M=10^{10}\,M_\odot$: $m_{bh,max}=1.3\times 10^{-20}$ eV
  - Solar mass BH $M=1\,M_\odot$: $m_{bh,min}=1.3\times 10^{-10}$ eV
- QCD axion $m\approx \Lambda_{QCD}^2/f_a$
  - $f_a=10^{16}$ GeV: $m\sim 10^{-9}$ eV
  - $f_a=10^{12}$ GeV: $m\sim 10^{-5}$ eV

Cf. $m_a = 1\mathrm{eV}\times\left(\frac{6\times 10^6\,\mathrm{GeV}}{f_a}\right)$

Contents

Axionic Superradiance Instability of Black Holes

Superradiance

Scalar field around a Kerr BH

$$(\Box - \mu^2)\Phi = 0; \quad \Phi \propto e^{-i\omega t + im\phi}$$

KG flux across the future horizon

$$k = \xi + \Omega_h \eta; \quad \xi = \partial_t, \quad \eta = \partial_\phi$$

$$I_{\mathscr{H}^+} = \int_{\mathscr{H}^+} (ik^\mu)\Phi^* \overleftrightarrow{\partial}_\mu \Phi = (\omega - \Omega_h m)\,|C|^2$$

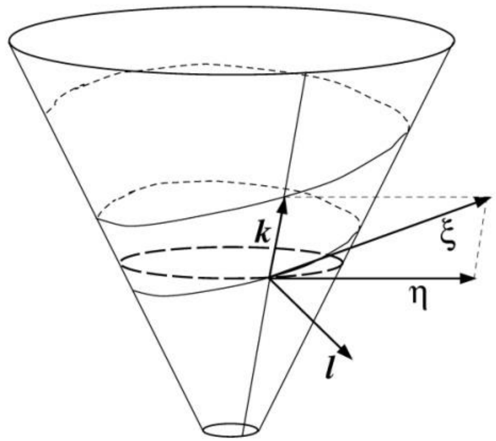

Flux across the horizon can become negative !!

Superradiance

$$\omega|A|^2_{\mathscr{I}^+} + (\omega - \Omega_h m)|C|^2 = \omega|A|^2_{\mathscr{I}^-}$$

$$\omega - m\Omega_h < 0 \Rightarrow \quad I_{\mathscr{I}^+} > I_{\mathscr{I}^-}$$

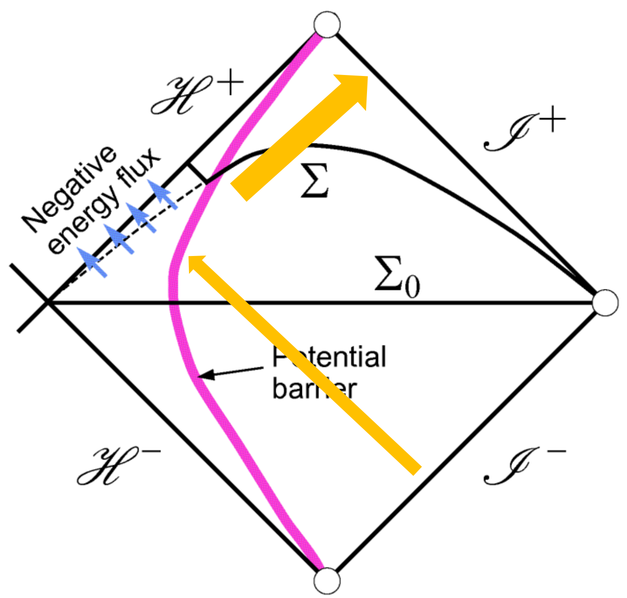

Superradiance Instability

Bound state modes of a massive scalar field around a Kerr BH become unstable due to superradiance.

[Damour, Deruelle, Ruffini (1976)]

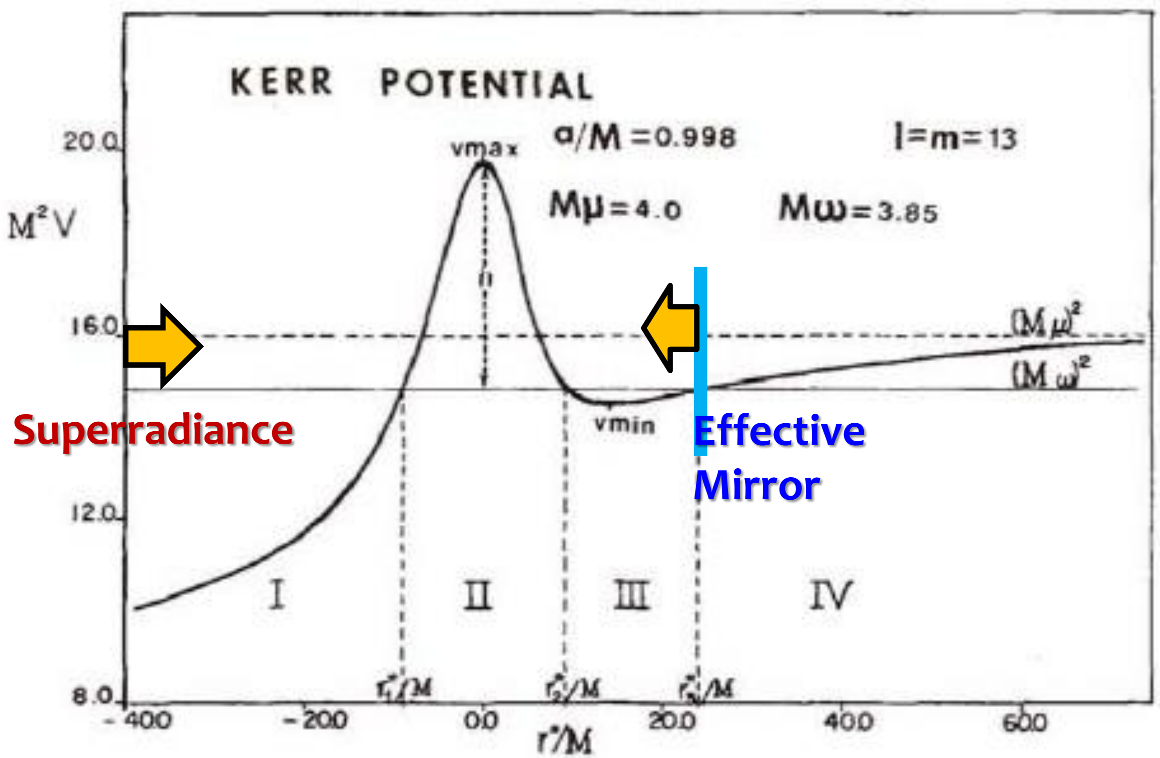

Zouros TJM, Eardley DM 197

Effective potential for P(r)

$$\Phi = P(r) S_l^m(\theta) e^{-i\omega t + im\phi} \quad \Rightarrow \quad -\frac{d^2}{dr^{*2}} P + (V - \omega^2) P = 0$$

Instability Growth Rate

Analytic Estimates

[Zouras & Eardley (1979), Detwiler (1980)]

$$\frac{\tau}{M} \approx \begin{cases} 10^7 e^{1.84\alpha_g} & ;\alpha_g \gg 1,\ a/M = 1 \\ 24\left(\frac{a}{M}\right)^{-1}(\alpha_g)^{-9} & ;\alpha_g \ll 1, \end{cases} \qquad (\alpha_g = \mu M)$$

General Features

- The growth rate is greatest for Mμ <0.5.
- The mode with l=m=1 is most unstable:
- The maximum growth rate at a=0.99 is

$$\tau \sim 10^7 M$$

$$M_\odot \quad \Rightarrow \quad \tau \sim 1\text{minute}$$

$$10^6 M_\odot \quad \Rightarrow \quad \tau \sim 2\text{years}$$

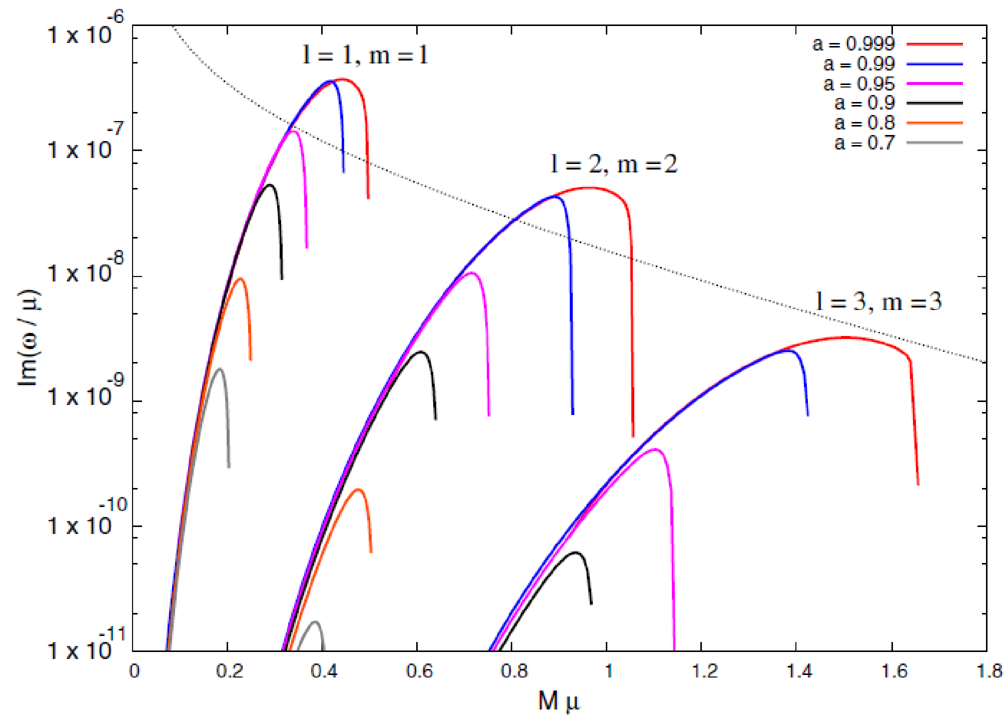

Dolan SR(2007)PRD76,084001

G-Atom

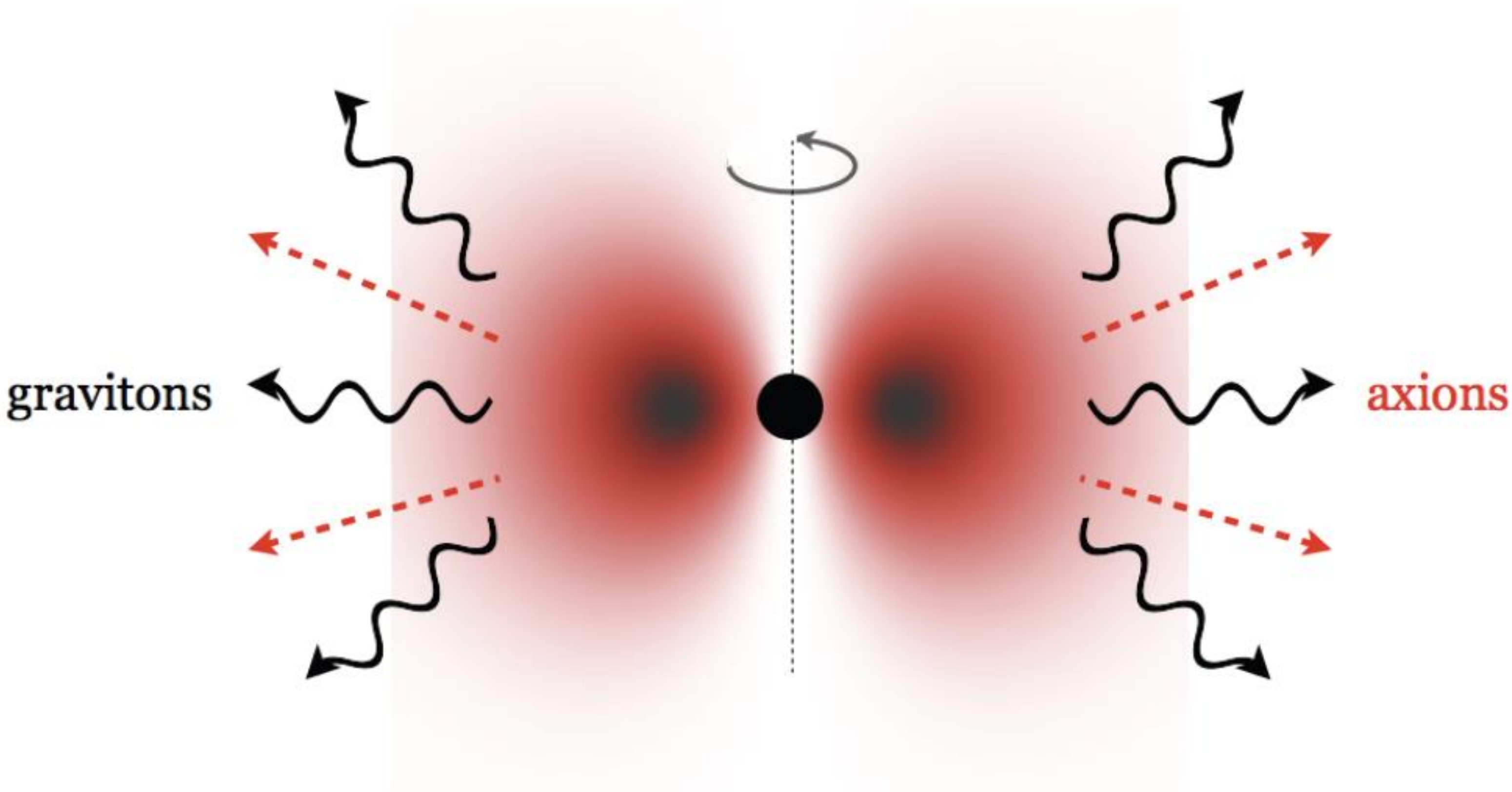

Arvanitaki A, Dubovsky S:
arXiv:1004.3558

Fate of G-Atom?

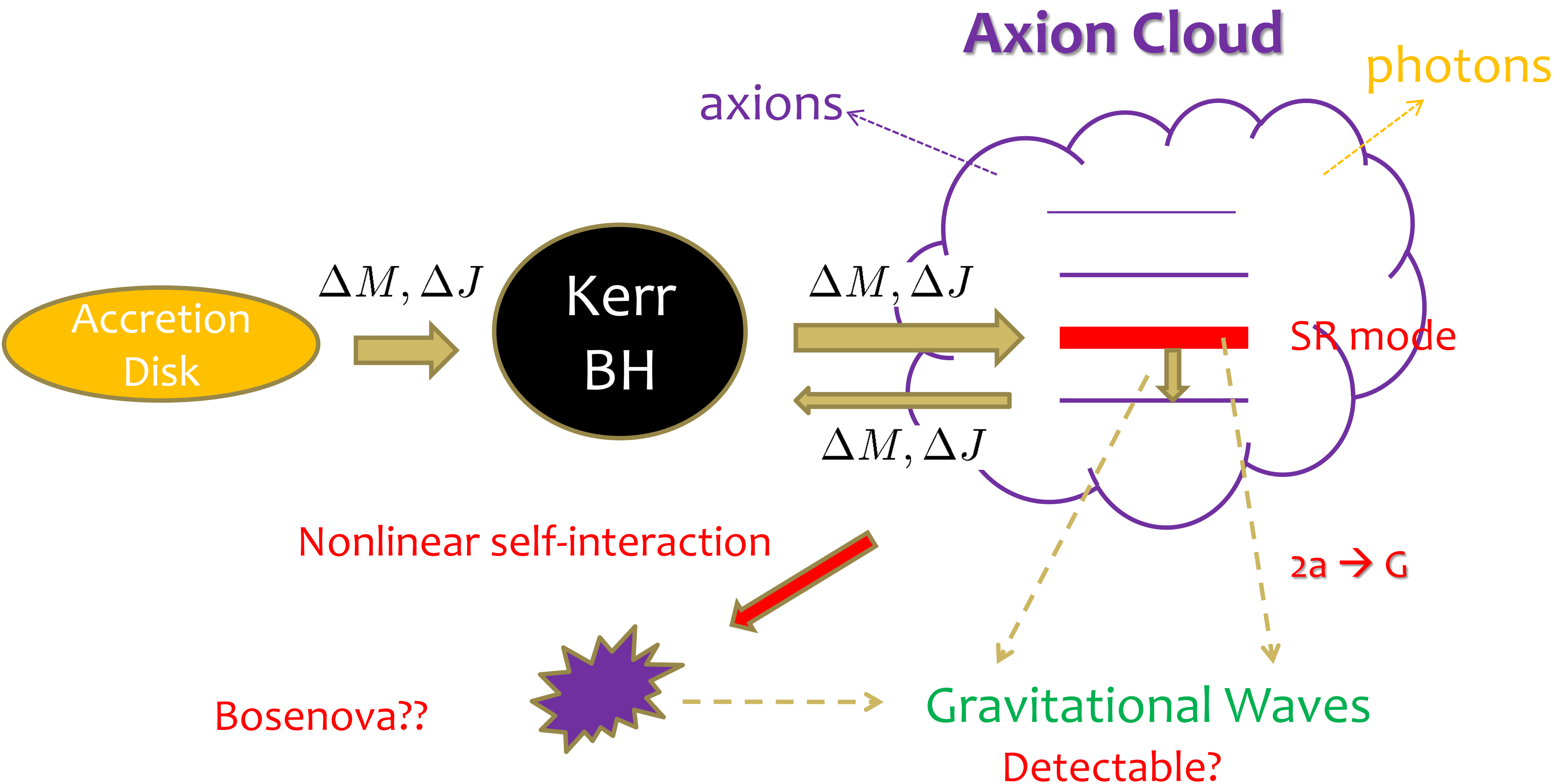

Axionic Bose Nova

Non-linear Effects

Action of the axion field

$$S = \int d^4x \sqrt{-g} \left[-\frac{1}{2}(\nabla\Phi)^2 - \frac{\mu^2 f_a^2}{2} \sin^2(\Phi/f_a) \right]$$

Estimation by Non-relativistic Approximation

$$\Phi \simeq \frac{1}{\sqrt{2\mu}} \left(e^{-i\mu t}\psi + e^{i\mu t}\psi^* \right)$$

Averaging S over a time scale >> 1/μ

$$S_{\rm NR} = \int d^4x \left[i\psi^* \partial_t \psi - \frac{1}{2\mu} \partial_i \psi \partial_i \psi^* - \mu \Phi_g \psi^* \psi + \frac{1}{16 f_a^2} (\psi^* \psi)^2 \right]$$

Attractive interaction

$$\propto E_a^2$$

Behavior of the Energy Flux into BH

Our direct 3D simulations reproduced the SR instability growth rate obtained by the Leaver method with sufficient precisions.

l=m=1 case

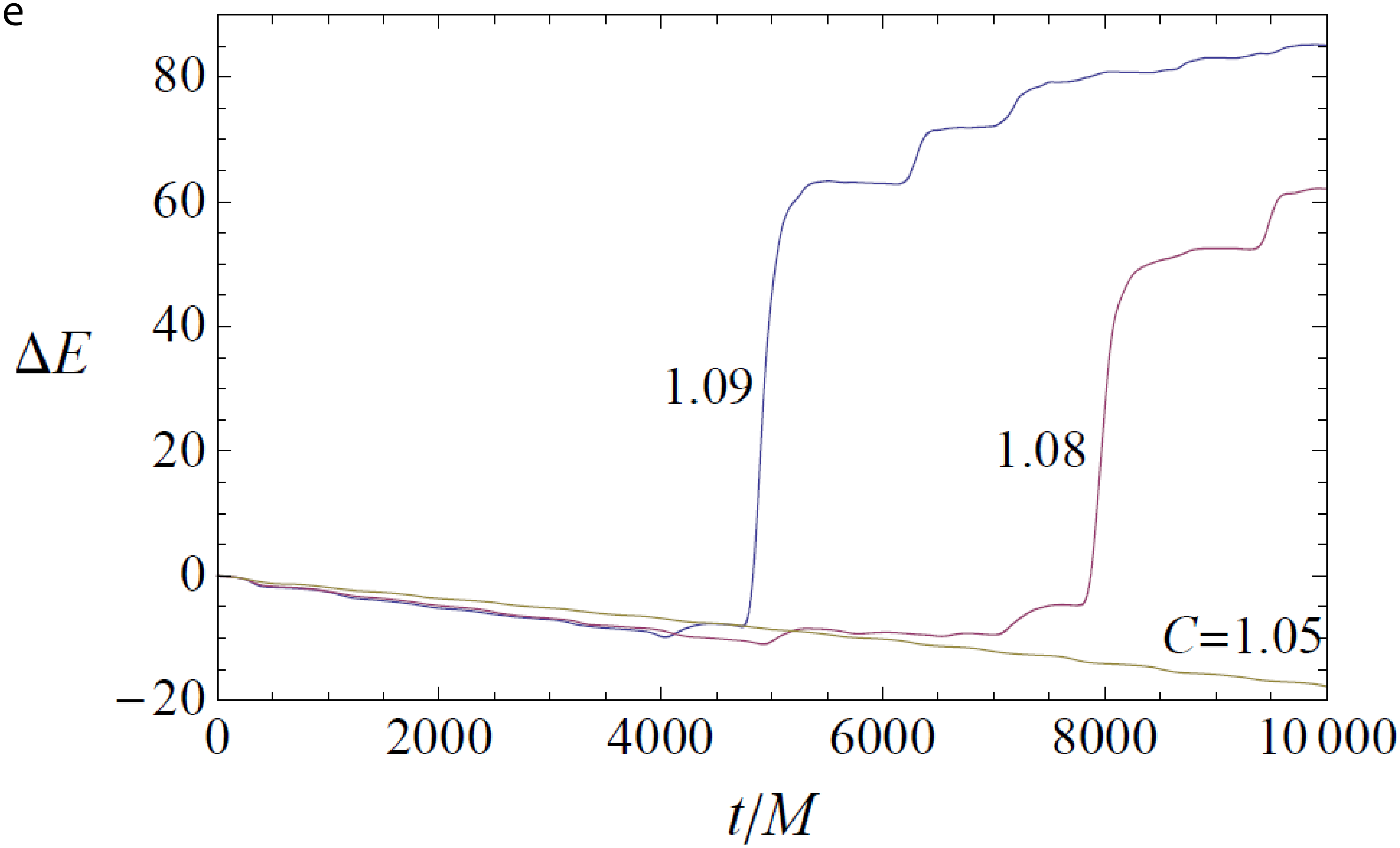

Full Relativistic 3D Numerical Simulations

Example: l=m=2 mode

- Parameters: $a/M = 0.99, \quad M\mu = 0.89$

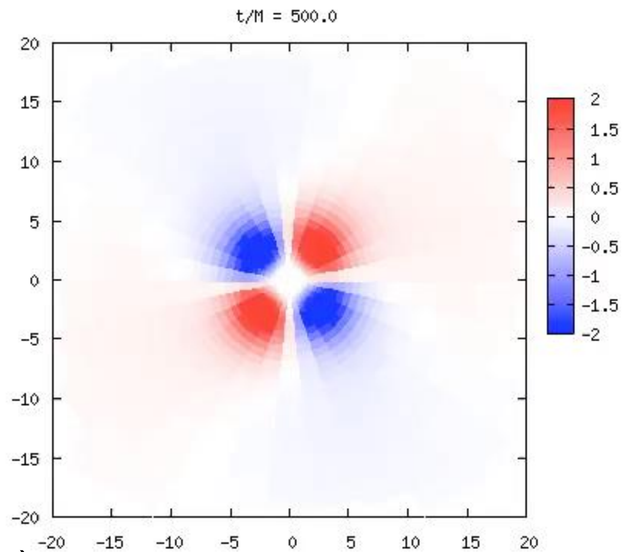

$r\sin\phi$

(Equatorial plane)

$r\cos\phi$

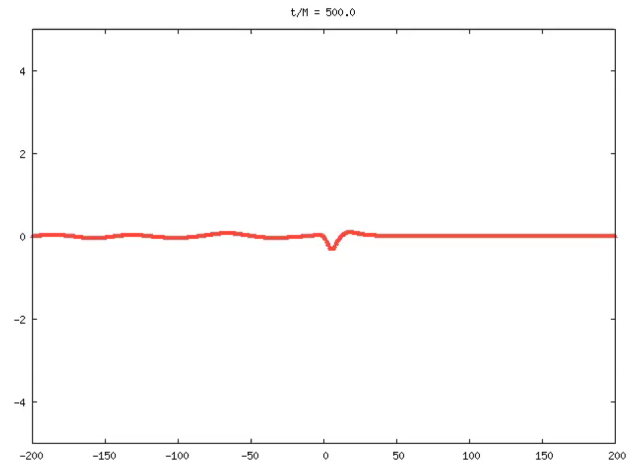

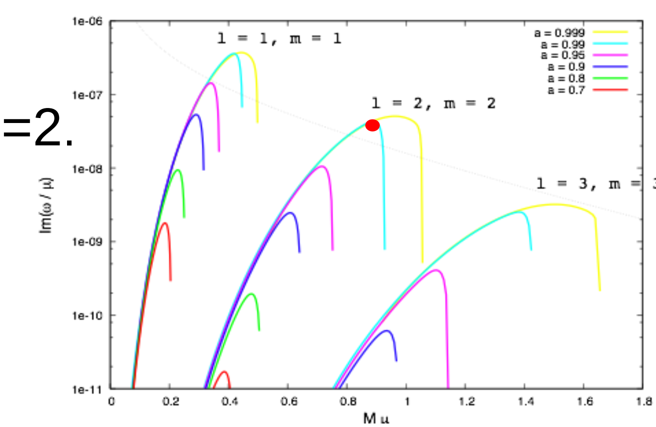

- Initial condition: the mode with l = m = 2, n=2.
- Initial amplitude: $\Phi/f_a = 0.7$

Summary of the Simulation: l=m=2

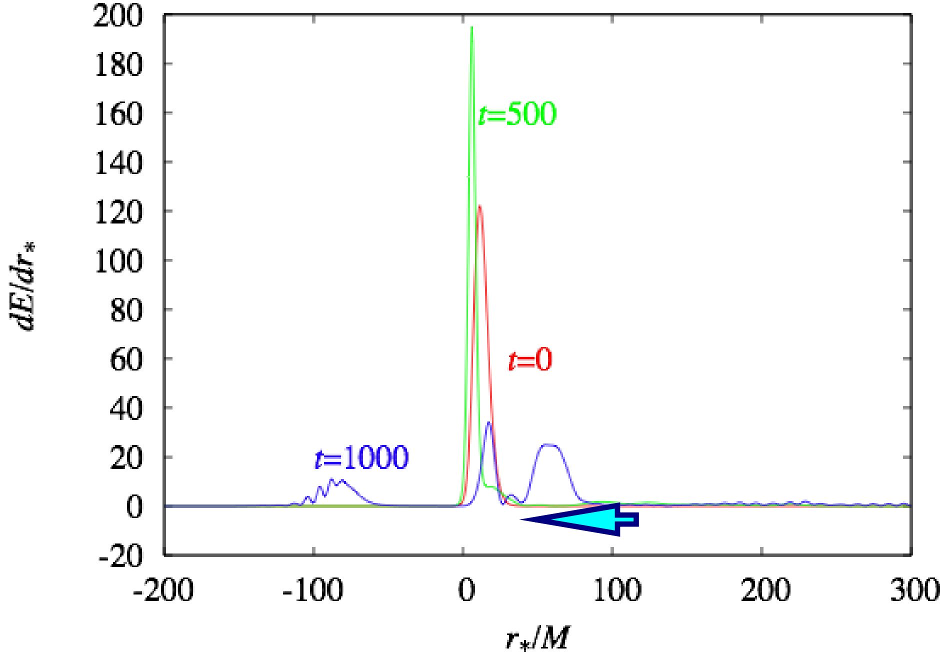

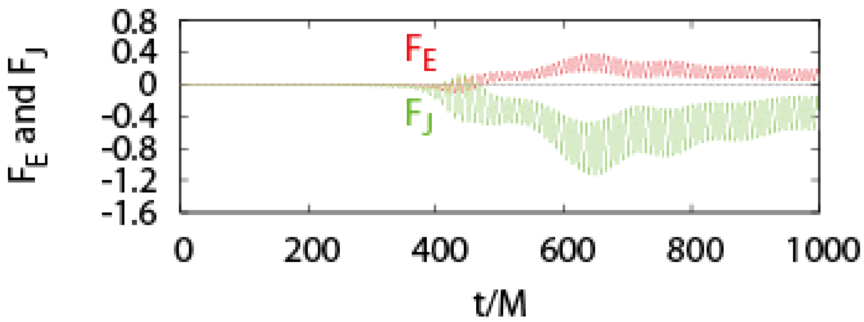

- When the peak value is sufficiently large, fairly large amount of axion cloud (20% of total energy) suddenly falls into the black hole in a relatively short time scale.

- This "bosenova implosion" occurs when

$$E_a/M \approx 10^{-3}(f_a/10^{16}\mathrm{GeV})^2 \Longleftrightarrow |\Phi_{\max}(0)/f_a| \sim 0.72$$

Gravitational Wave Emissions

Does the GW Emission Stop Instability?

Estimation by Quadrupole Formula

$$r_c \simeq \frac{l+1}{\mu\alpha_g}, \quad \Omega \simeq \sqrt{\alpha_g}\mu r_c^3$$

$$\Rightarrow \quad P_Q = \frac{G}{45}|\dddot{Q}|^2 \sim \frac{G}{45}(r_c^2\epsilon M)^2\Omega^6 \sim \frac{\epsilon^2\alpha_g^{10}}{45G(l+1)^{10}} \qquad \left(\epsilon = \frac{E_a}{M}\right)$$

GW emission vs SR instability growth

$$\dot{E}_{\rm SR} = C_{\rm SR}(\alpha_g, a)(E_a/M) \propto E_a$$

$$\dot{E}_{\rm GW} = -C_{\rm GW}(\alpha_g, a)(E_a/M)^2 \propto -E_a^2$$

$$\Rightarrow \quad \frac{|\dot{E}_{\rm GW,Q}|}{\dot{E}_{\rm SR}} \approx 2\times 10^5 \epsilon \left(\frac{\alpha_g}{l+1}\right)^{10}$$

$$\approx 0.02\epsilon \quad (l=1, \alpha_g = 0.4)$$

For superradiant modes, however, level transitions are in general suppressed, and 2 axions -> graviton process is dominant.

We have to estimate the GW emission rate by this 2 axions -> graviton process.

GW Energy Flux Formula in a Kerr Background

- The formula for evaluating the amplitude

$$\triangle_L \psi_{\mu\nu} = 16\pi G T_{\mu\nu}$$

$$\int_{\partial D} \left(h^*_{ab} \nabla_c \psi^{ab} - \psi^{ab} \nabla_c h^*_{ab} \right) n^c d\Sigma = -16\pi G \int_D h^*_{ab} T^{ab} \sqrt{-g} d^4 x$$

Physical perturbation

Homogeneous solution

- Rate of GW energy emission/absorption

$$\dot{E}_{\mathscr{I}^+} = 2\pi G \sum_{l,m,s,\tilde{\omega}} |C^s_{lm}|^{-2} \, |\langle u_{lms\,\tilde{\omega}}, T \rangle|^2$$

$$\langle u, T \rangle := \frac{1}{\Delta t} \int_D d^4 x \sqrt{-g} u^{\mu\nu} T_{\mu\nu}$$

$$\Box u_{\mu\nu} = 0; \quad u^\mu_\mu = 0, \quad \nabla_\nu u^\nu_\mu \sim 0 \text{ at } \mathscr{I}^+$$

$$\boxed{\Phi, \quad u_{\mu\nu} \Rightarrow \quad \dot{E}_{\mathscr{I}^+}}$$

Teukolsky equations + Chrzanowski formula

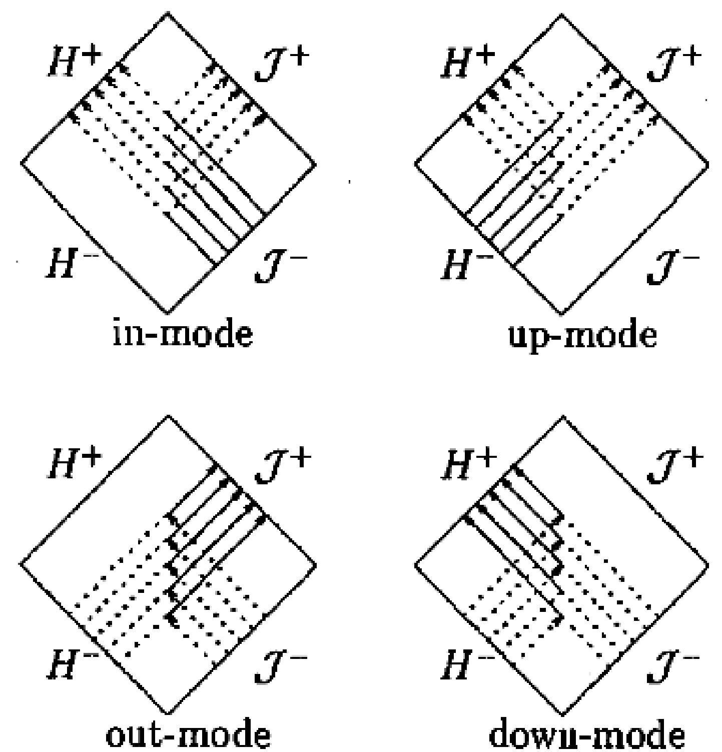

Axion cloud in l = m = 2 mode

- ○ $(\tilde{\ell}, \tilde{m}) = (4, 4), \ (P = +1)$
- ● $(\tilde{\ell}, \tilde{m}) = (5, 4), \ (P = -1)$
- □ $(\tilde{\ell}, \tilde{m}) = (6, 4), \ (P = +1)$
- ■ $(\tilde{\ell}, \tilde{m}) = (7, 4), \ (P = -1)$

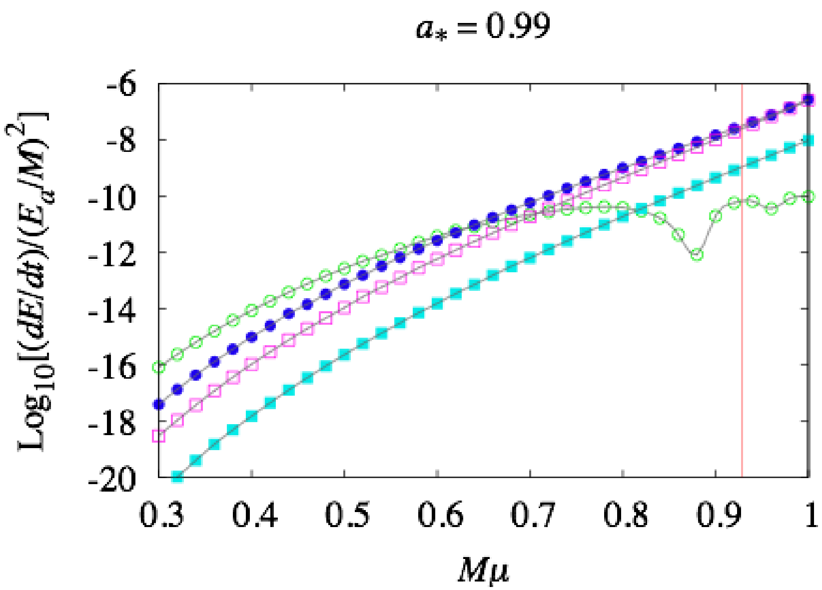

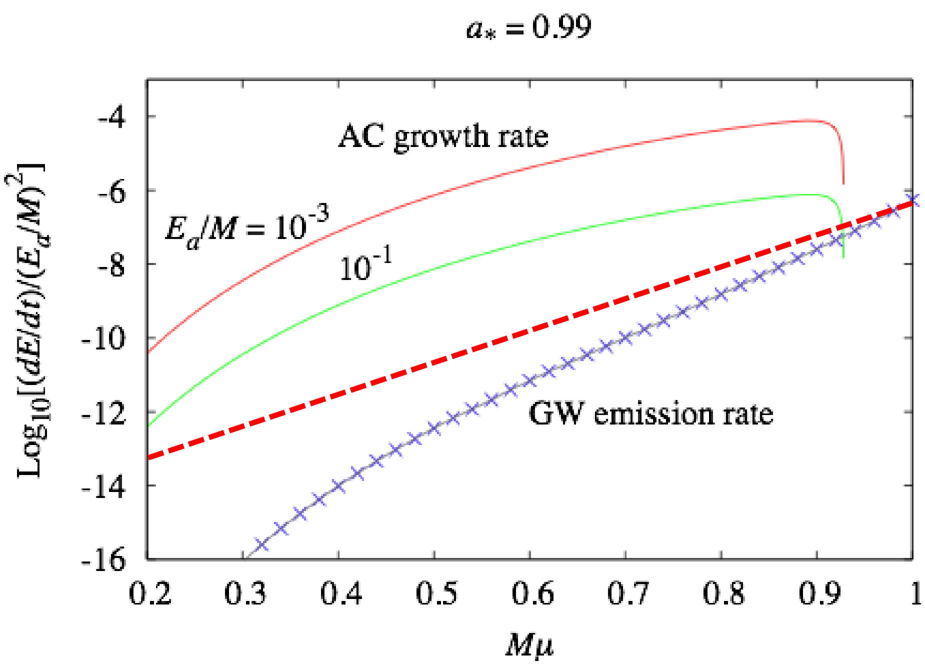

GW emissions do not hider the occurrence of the bose nova collapse!!

Can We Observe GWs from Axion Bosenova?

Estimation by Quadrupole Formula

$$h \approx 8 \times 10^{-23} \left(\frac{\epsilon}{10^{-3}}\right) \left(\frac{c^3}{GM\omega}\right) \left(\frac{10\mathrm{kpc}}{d}\right) \left(\frac{M}{10M_\odot}\right) \left(\frac{3\alpha_g}{l+1}\right)^5$$

$$\approx 8 \times 10^{-21} \left(\frac{\epsilon}{10^{-3}}\right) \left(\frac{c^3}{GM\omega}\right) \left(\frac{10\mathrm{Mpc}}{d}\right) \left(\frac{M}{10^6 M_\odot}\right) \left(\frac{3\alpha_g}{l+1}\right)^5$$

Examples

- **Cygnus X-1**

$$M = 14.8 \pm 1.0 M_\odot, \quad a/M \gtrsim 0.9$$

$$d = 1.86\mathrm{kpc}$$

$$\Delta t \approx 100M \approx 7.3 \text{ ms}$$

$$\Rightarrow \quad h\Delta t^{1/2} \approx 10^{-23}\mathrm{Hz}^{-1/2}$$

$$(\alpha_g = 0.7, \quad l = 2)$$

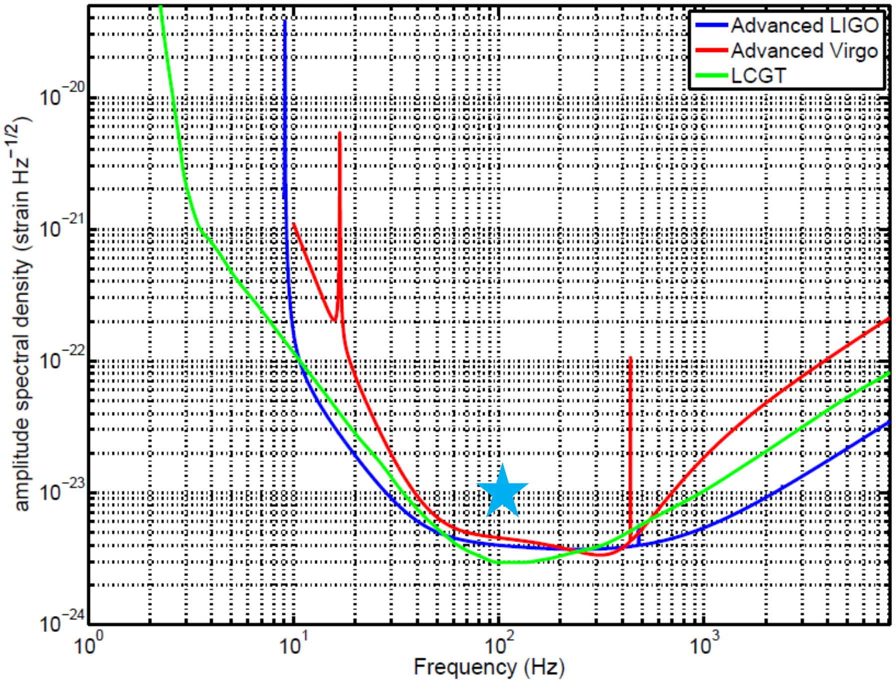

- **Sagitairus A***

$$M \approx 10^6 M_\odot, \quad d \approx 8\mathrm{kpc}$$

$$\Delta t \approx 100M \approx 500 \text{ s}$$

$$\Rightarrow \quad h\Delta t^{1/2} \approx 10^{-17}\mathrm{Hz}^{-1/2}$$

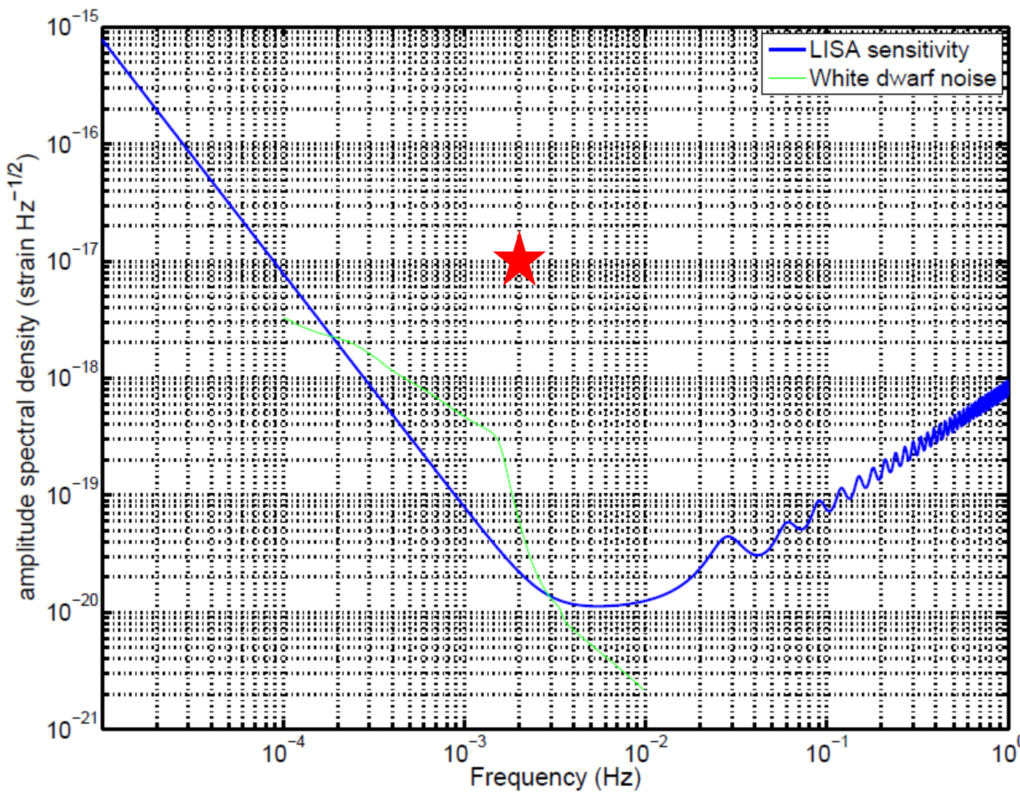

GWs during the SR Growth Phase

- For stationary GWs, we can gain S/N by long time observations.

When the duration of observation/SR phase is T, and the frequency range of the GWs is $\Delta\nu$, the S/N is

$$\mathscr{S}/\mathscr{N} \approx \frac{h^2 T}{\hat{N}(\omega)} \times \min\left(1, \frac{1}{(T\Delta\nu)^2}\right)$$

- Cygnus X-1

$$T \sim 10^7 M \sim 10^3 \mathrm{s}$$

$$h \sim 10^{-22} \ (l=1, \alpha_g = 0.5)$$

$$\nu \approx \mu/\pi \sim 2 \times 10^3 \mathrm{Hz}$$

if $T\Delta\omega<1$, then

$$h\sqrt{T} \approx 3 \times 10^{-21} \mathrm{Hz}^{-1/2}$$

LIGO sensitivity (2012)

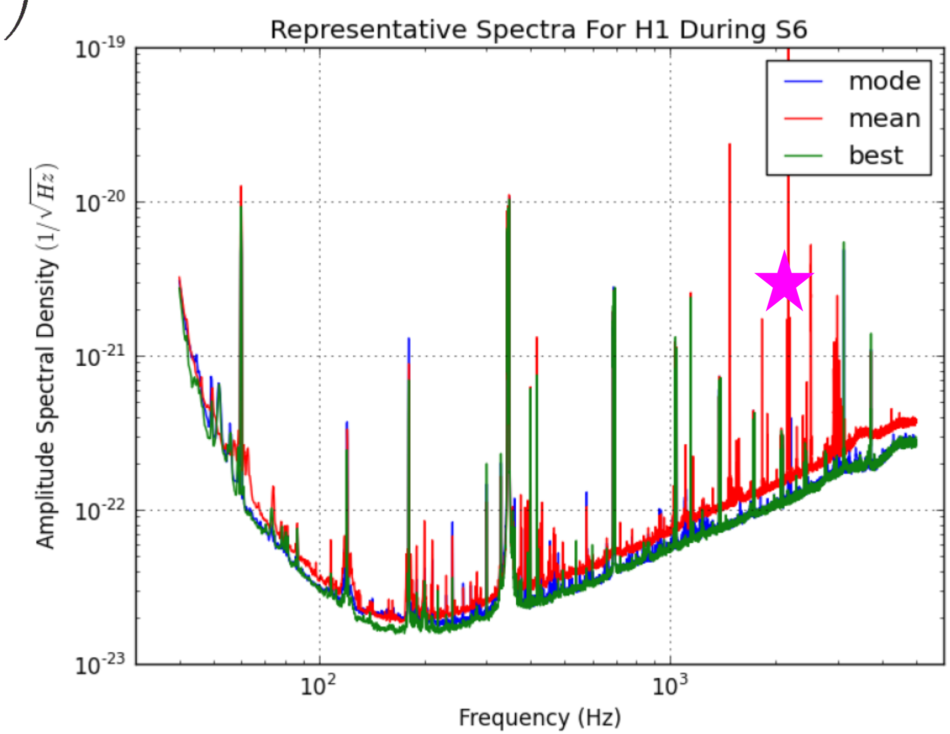

Axion cloud in l = m = 1 mode

- $(\tilde{\ell}, \tilde{m}) = (2,2), \ (P=+1)$
- $(\tilde{\ell}, \tilde{m}) = (3,2), \ (P=-1)$
- $(\tilde{\ell}, \tilde{m}) = (4,2), \ (P=+1)$
- $(\tilde{\ell}, \tilde{m}) = (5,2), \ (P=-1)$

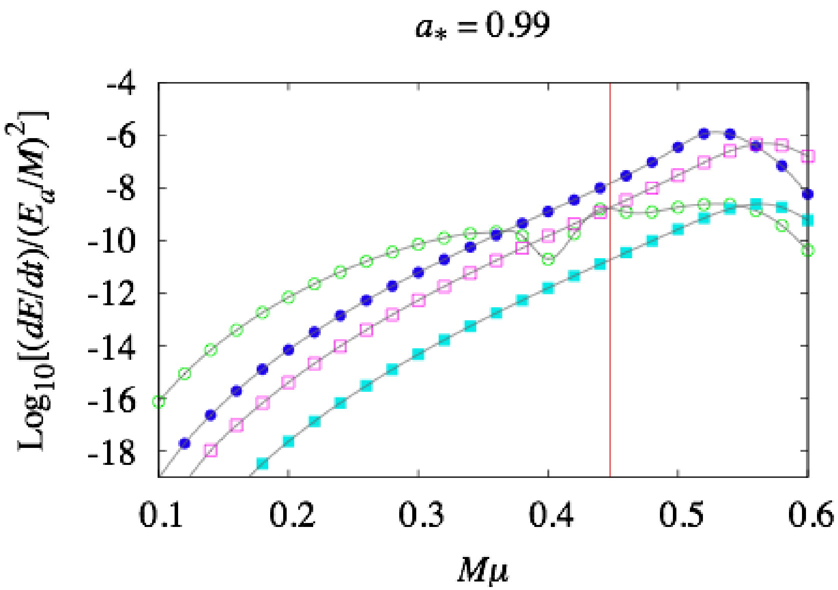

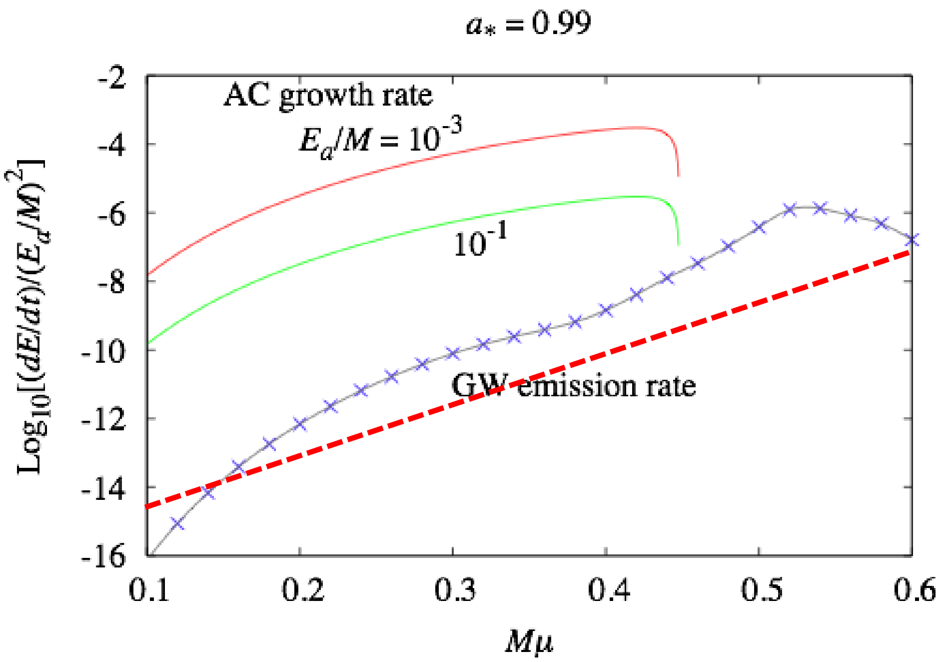

Caveat

- When the axion cloud grows, nonlinear effects become important and produce modulations with intermediate periods.
- This modulation produces a frequency dispersion

$$\Delta\nu \sim \frac{1}{\Delta T} \sim \frac{1}{1000M} \sim \frac{10^4}{T}$$

$$\frac{h\sqrt{T}}{T\Delta\nu} \sim 3 \times 10^{-25}\mathrm{Hz}^{-1/2}$$

- This difficulty will be resolve by the matched filtering to simulations.

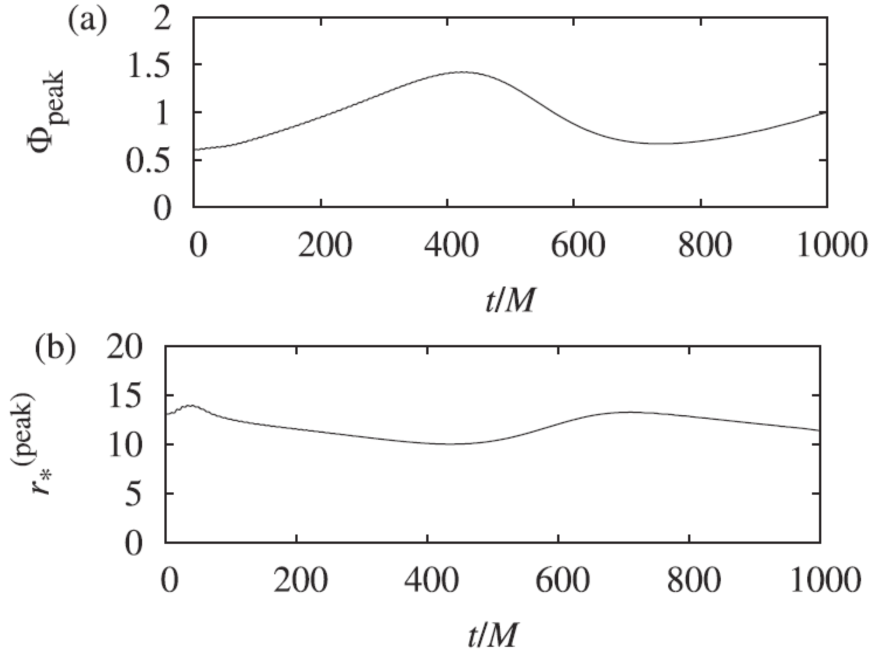

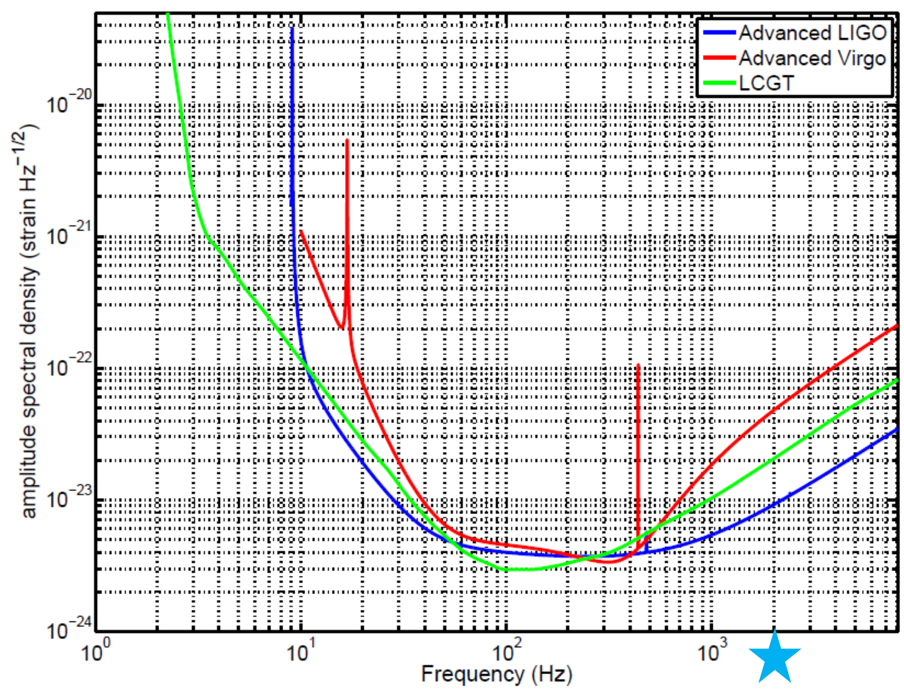

Gamma Ray Astropysics vs CIRB

Gamma-Ray Horizon

Optical depth against CBR

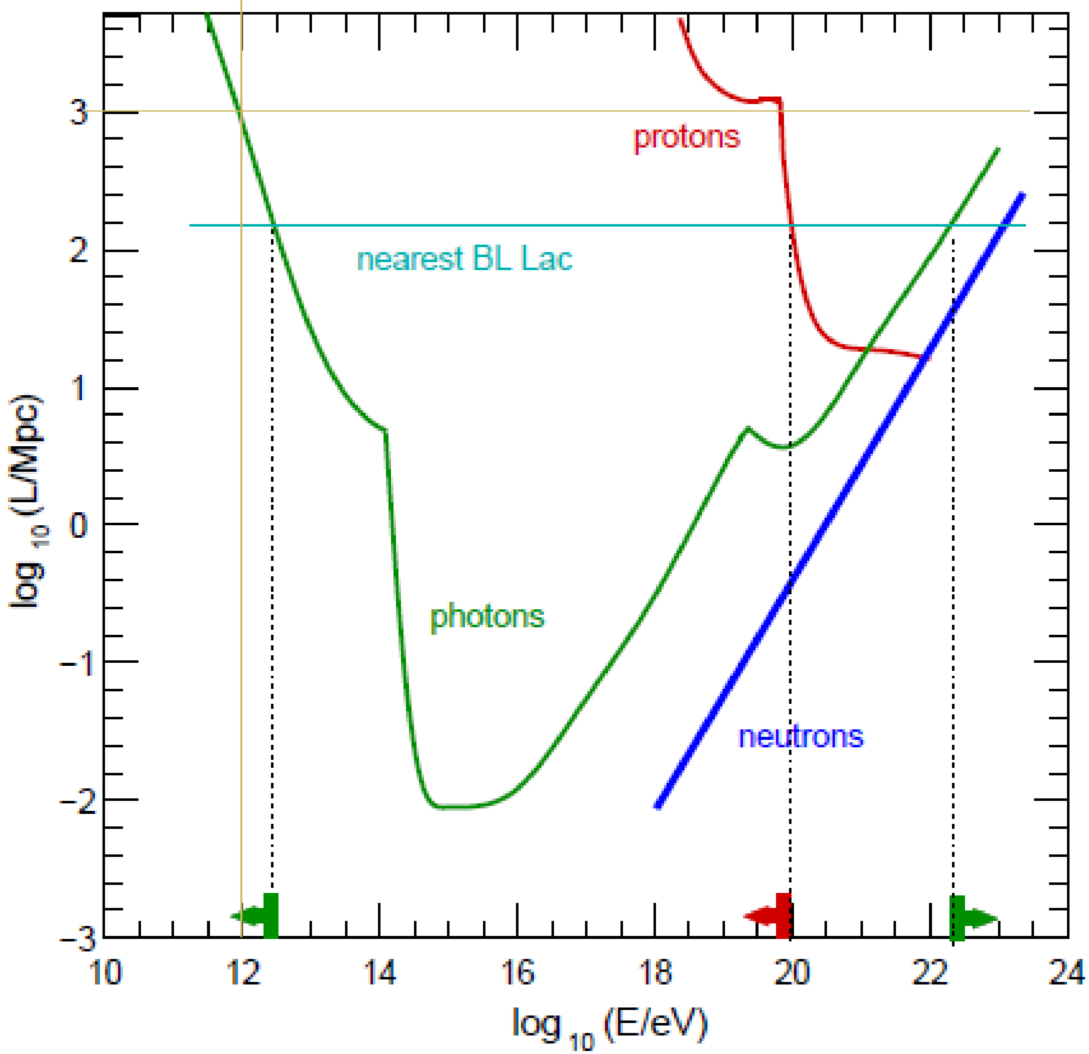

GZK cut-off

$$p + \gamma \rightarrow p + \pi^0,\ n + \pi^+$$

$$E_p \gtrsim 10^{20}\mathrm{eV}$$

γ–γ opacity

$$\gamma + \gamma \rightarrow e^+ + e^-$$

$$\omega_{\mathrm{HE}\gamma} \geq \frac{2.5\times10^{11}\mathrm{eV}^2}{\omega_{\mathrm{BG}\gamma}}$$

Fairbairn, Rashba, Troitsky: PRD84, 25019 (2011); Roncadelli, de Angelis, Mansutti 2009

Deformation of the Gamma Ray Spectrum

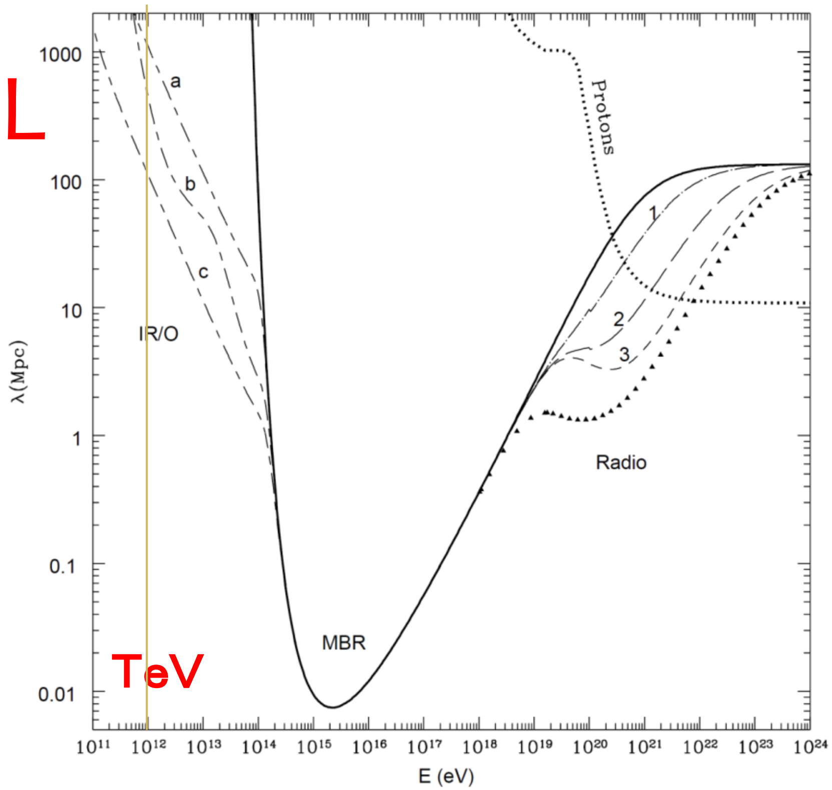

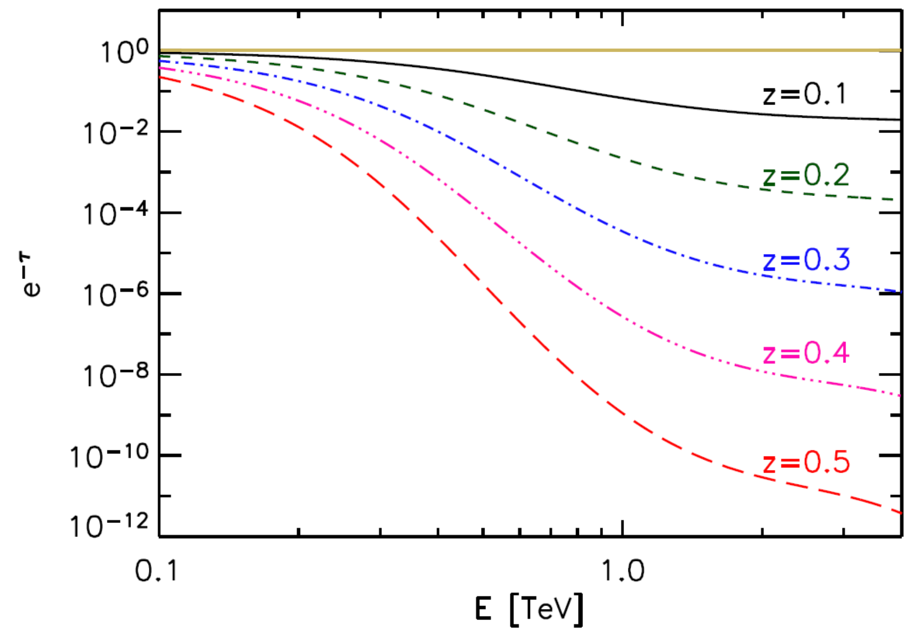

M Simet, D Hooper, PD Serpico:
PRD 77, 063001 (2008)

PS Coppi and AF Aharonian:
ApJ 487, L9 (1997).

z=0.1 ⇔ L≃ 430 Mpc

$$a \quad : \quad \epsilon^2 n(\epsilon,0) = 10^{-3}\mathrm{eV/cm}^3$$

$$c \quad : \quad \epsilon^2 n(\epsilon,0) = 10^{-2}\mathrm{eV/cm}^3$$

$$\text{Cf.} \ \ \rho_{\mathrm{CMB}} = 0.26\,\mathrm{eV/cm}^3$$

Observation of EBL absorption in the spectra of AGNs

- HESS observation: power-law fitting
  - Two blazars with strong absorption were observed.
- Fermi-LAT observation: power-law fitting

  [Ackermann at al (Fermi Coll): Science 338, 1190 (2012)]

  The spectral deformation due to absorption has been observed for 150 blazars of BL Lac type.

  (z=0.03 -1.6, E= 40GeV – 100 GeV)
- Multi-frequency observation: synchrotron/SSC model

  [Dominguez et al: apj770, 88 (2013)]

  Opacity around a TeV range is determined by observations of 15 blazars from radio to Gamma-ray (Fermi-LAT & IACTs).

  The opacity is consistent with the minimum EBL model.

  (z=0.031 – 0.5, E=200 GeV – 10 TeV)

Detection of the Absorption by Fermi

Sample: 150 blazers of BL Lac type (z=0.03 -1.6, E= 40GeV – 100 GeV)

Fig. 1. Measurement, at the 68 and 95% confidence levels (including systematic uncertainties added in quadrature), of the opacity $\tau_{\gamma\gamma}$ from the best fits to the Fermi data compared with predictions of EBL models. The plot shows the measurement at $z \approx 1$, which is the average redshift of the most constraining redshift interval (i.e., $0.5 \leq z < 1.6$). The Fermi-LAT measurement was derived combining the limits on the best-fit EBL models. The downward arrow represents the 95% upper limit on the opacity at $z = 1.05$ derived in (*13*). For clarity, this figure shows only a selection of the models we tested; the full list is reported in table S1. The EBL models of (*49*), which are not defined for $E \geq 250/(1 + z)$ GeV and thus could not be used, are reported here for completeness.

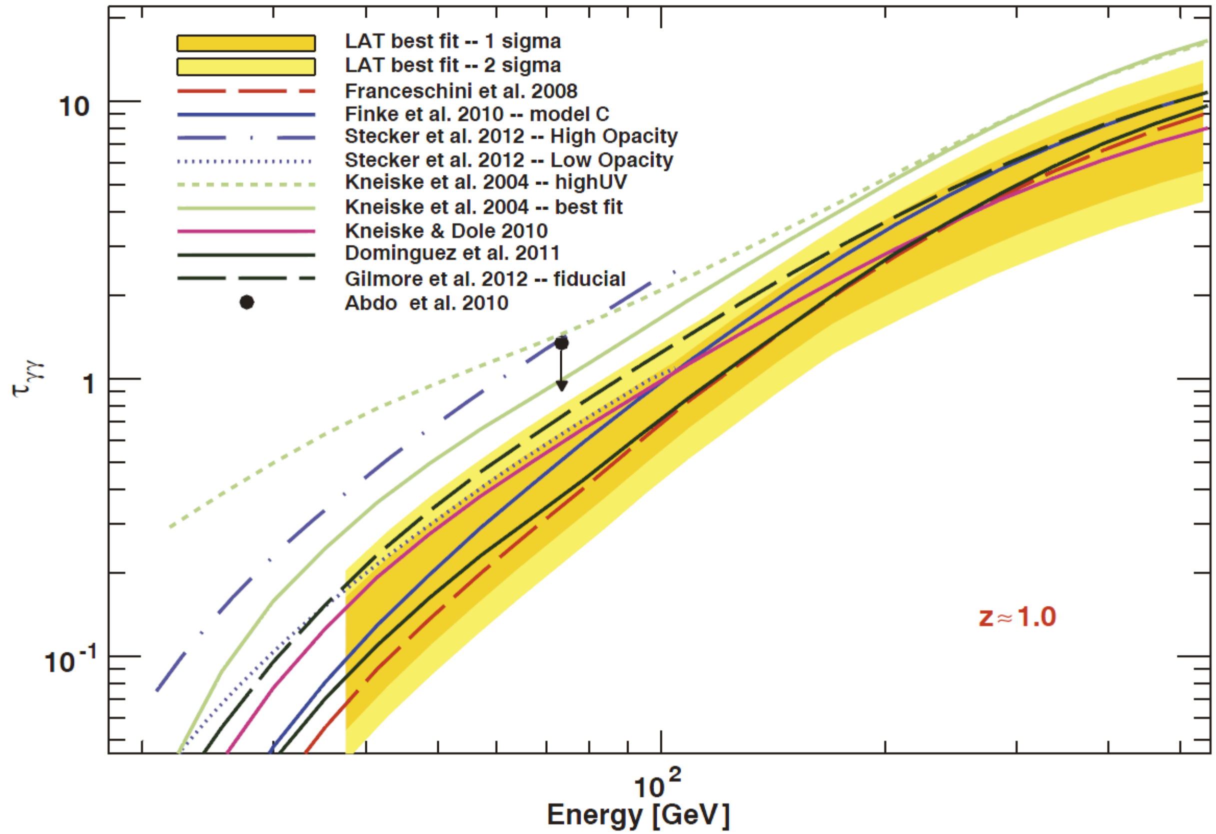

Ackermann at al (Fermi Coll): Science 338, 1190 (2012)

Rejection of the intrinsic origin

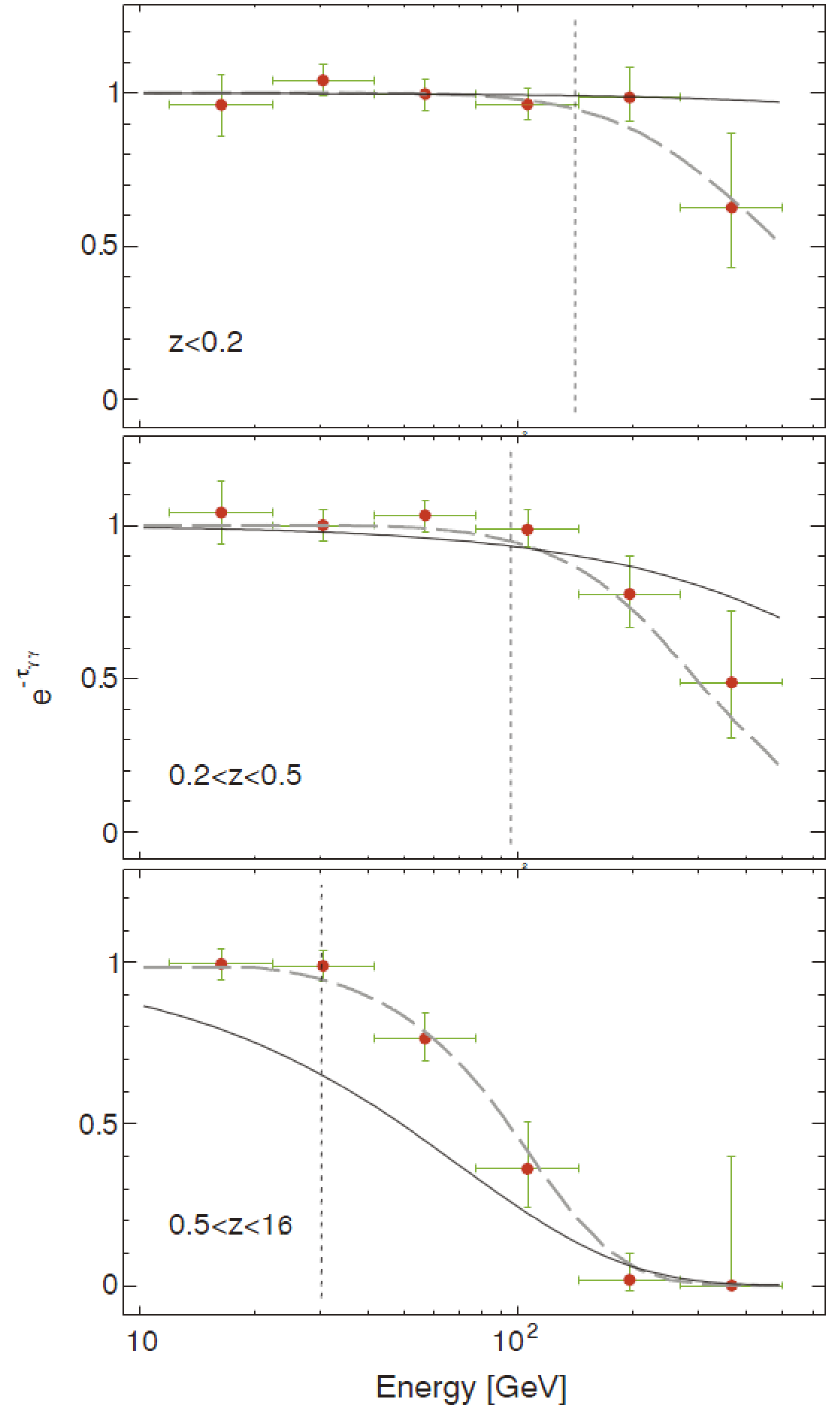

Fig. 2. Absorption feature present in the spectra of BL Lac objects as a function of increasing redshift (data points, from top to bottom). The dashed curves show the attenuation expected for the sample of sources by averaging, in each redshift and energy bin, the opacities of the sample [the model of (*7*) was used] and multiplying this average by the best-fit scaling parameter *b* obtained independently in each redshift interval. The vertical line shows the critical energy E_{crit} below which ≤ 5% of the source photons are absorbed by the EBL. The thin solid curve represents the best-fit model, assuming that all the sources have an intrinsic exponential cutoff and that blazars follow the blazar sequence model of (*32*, *33*).

Ackermann at al (Fermi Coll): Science 338, 1190 (2012)

Observed CGRH : E0(z)

Dominguez et al: apj770, 88 (2013)

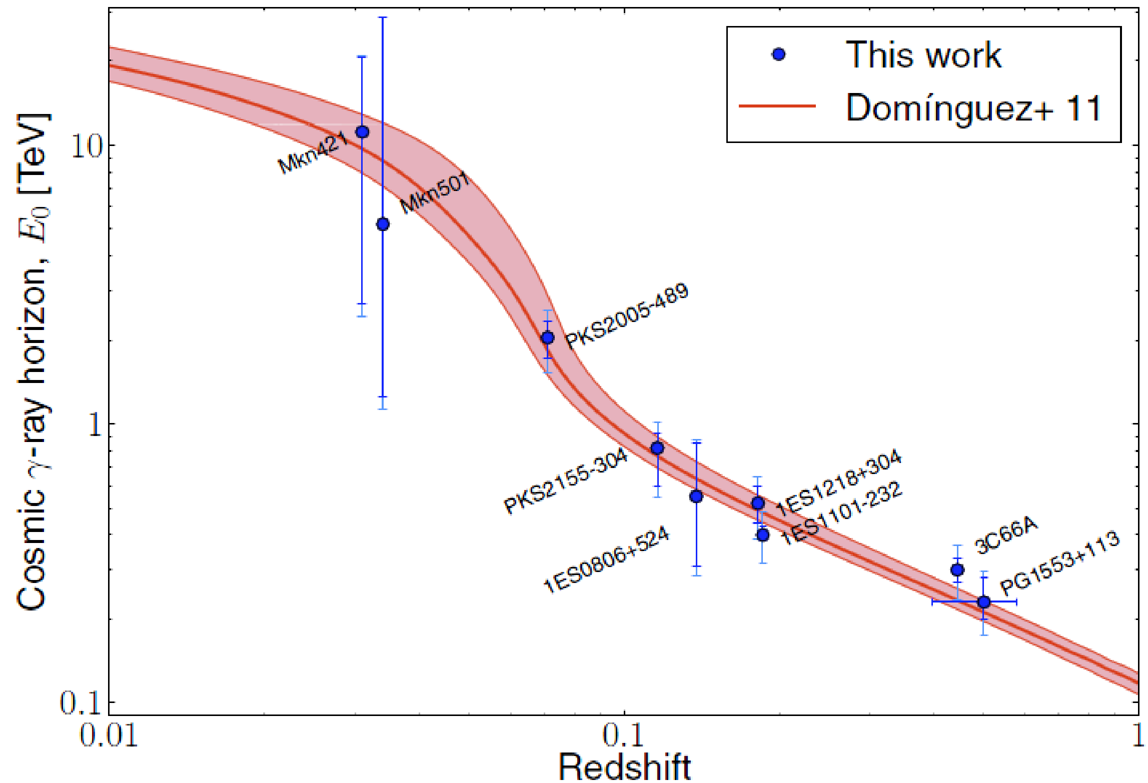

Figure 2. Estimation of the CGRH from every blazar in our sample plotted with blue circles. The statistical uncertainties are shown with darker blue lines and the statistical plus 20% of systematic uncertainties are shown with lighter blue lines. The CGRH calculated from the EBL model described in Domínguez et al. (2011a) is plotted with a red thick line. The shaded regions show the uncertainties from the EBL modeling, which were derived from observed data.

EBL models and measurements

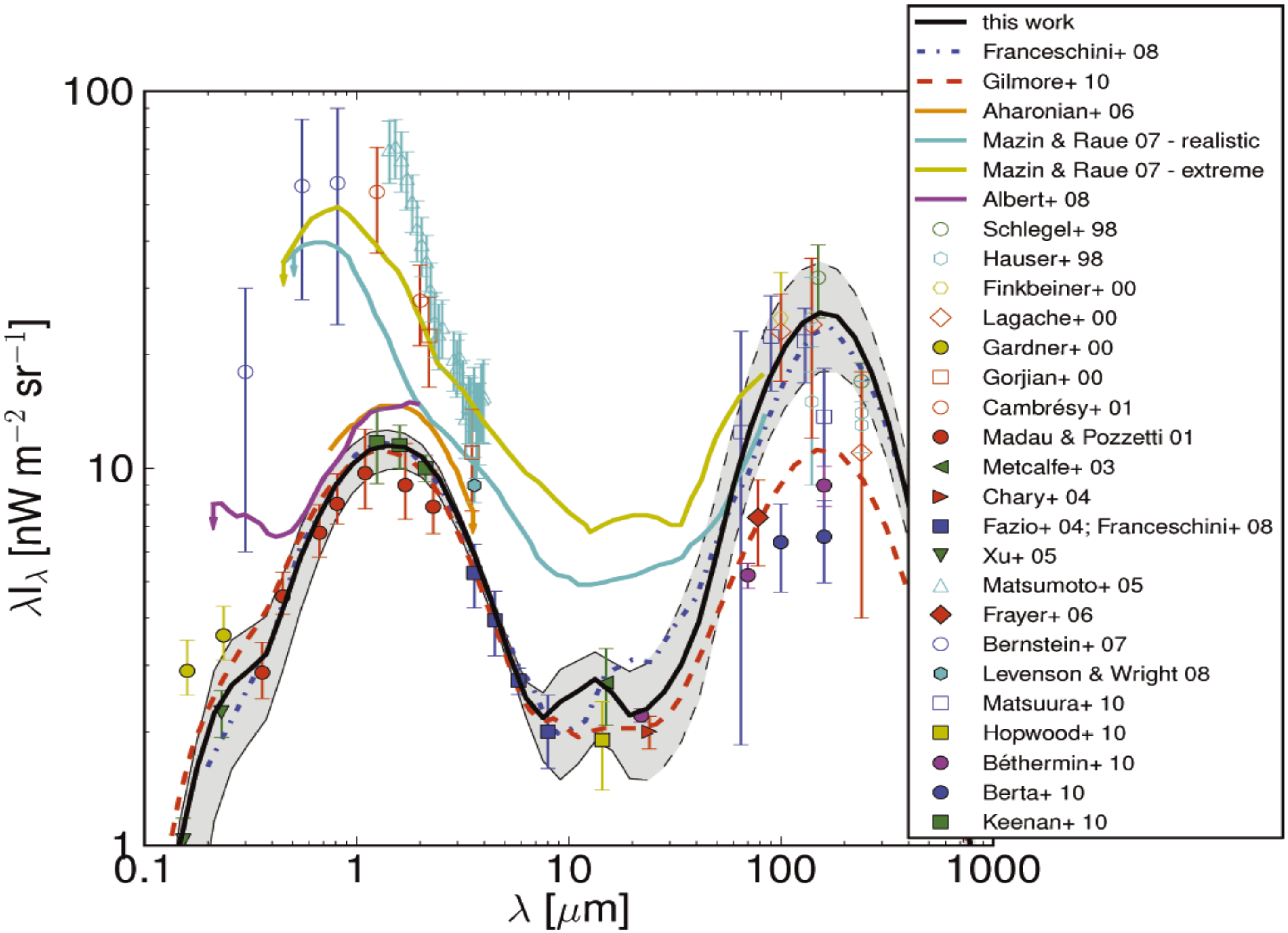

Dominguez A et al: mnras 410, 2556 (2011)

CIBER

CIBER

Cosmic Infrared Background ExpeRiment

JAXA ISAS

The CIBER Collaboration

JPL Jet Propulsion Laboratory, California Institute of Technology

John Battle
Jamie Bock
Viktor Hristov
Anson Lam
Phil Korngut
Peter Mason
Michael Zemcov

Asantha Cooray
Joseph Smidt
Matt Weiss

Brian Keating
Tom Renbarger

JAXA Japan Aerospace Exploration Agency

Shuji Matsuura
Toshiaki Arai
Kohji Tsumura
Mai Shirahata
Takehiko Wada

Seoul National University

Min Gyu Kim

Korea Astronomy and Space Science Institute

Dae Hee Lee
Uk Won Nam

ASIAA

Toshio Matsumoto

Axion Cosmophysics AIU2012, KEK, Nov 6-9, 2012

[From the slides of the talk by S Matsuura at AIU2012]

Observational limits on the NIR background

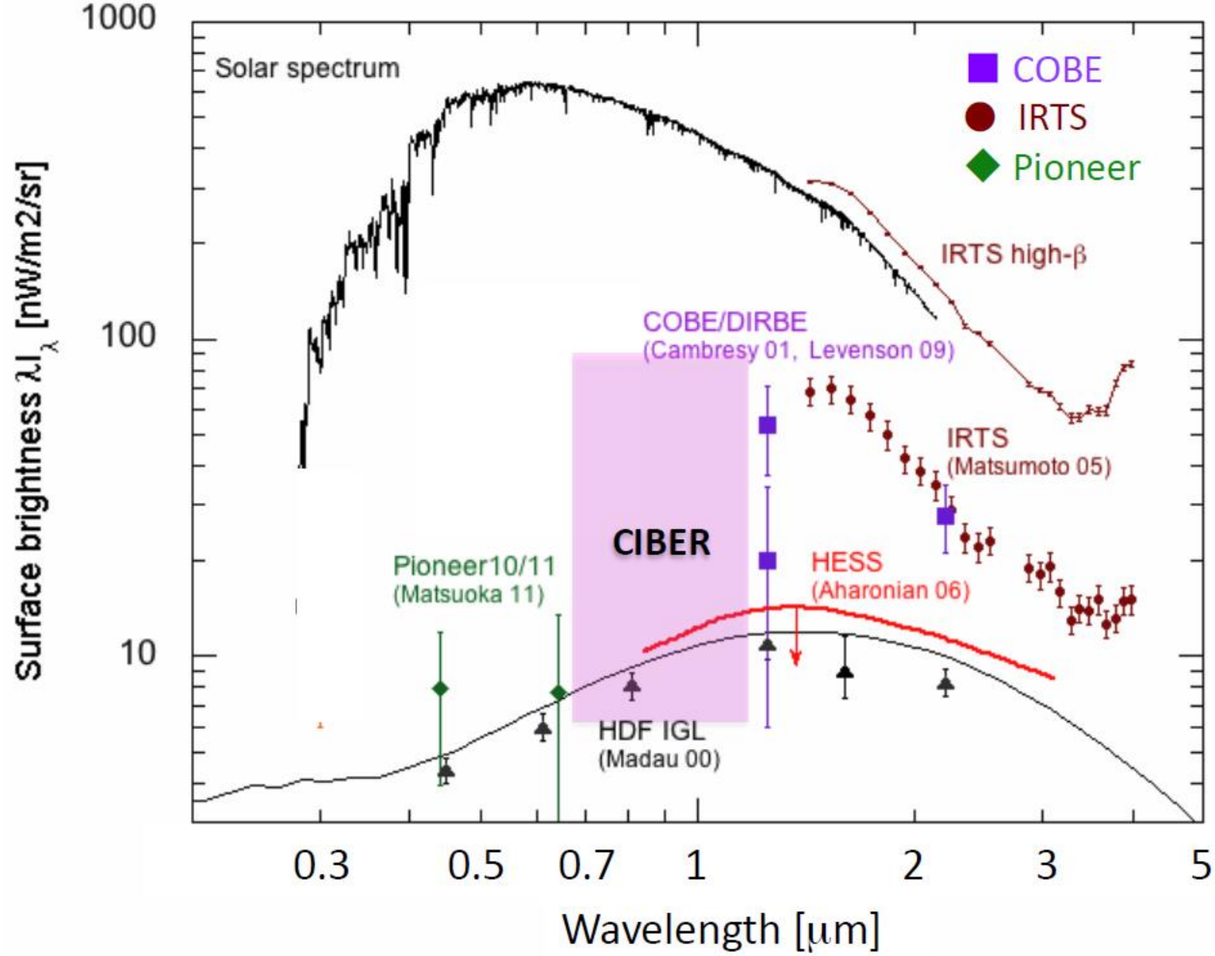

[From the slides of the talk by S Matsuura at AIU2012]

Zodiacal Light

- Scattered sun light by interplanetary dust
- Strong ecliptic latitude dependence

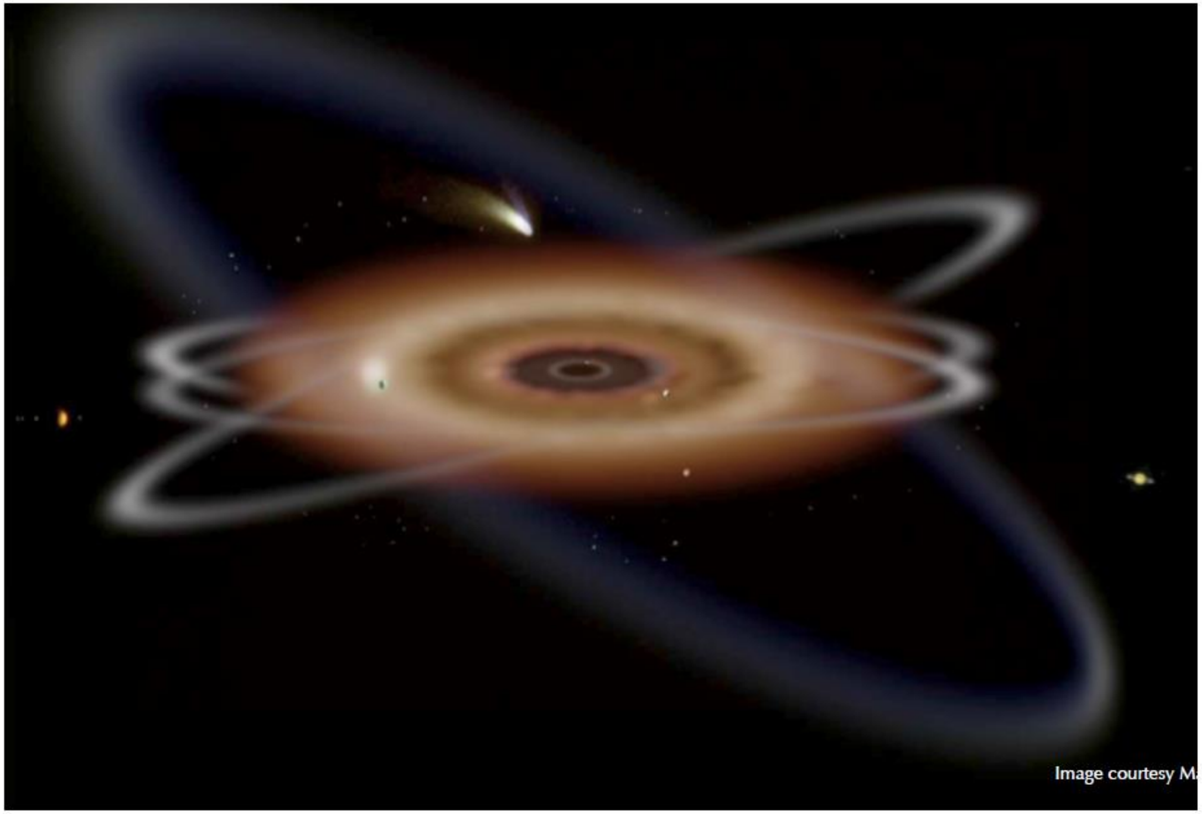

[From the slides of the talk by S Matsuura at AIU2012]

The Cosmic Infrared Background ExpeRiment (CIBER)

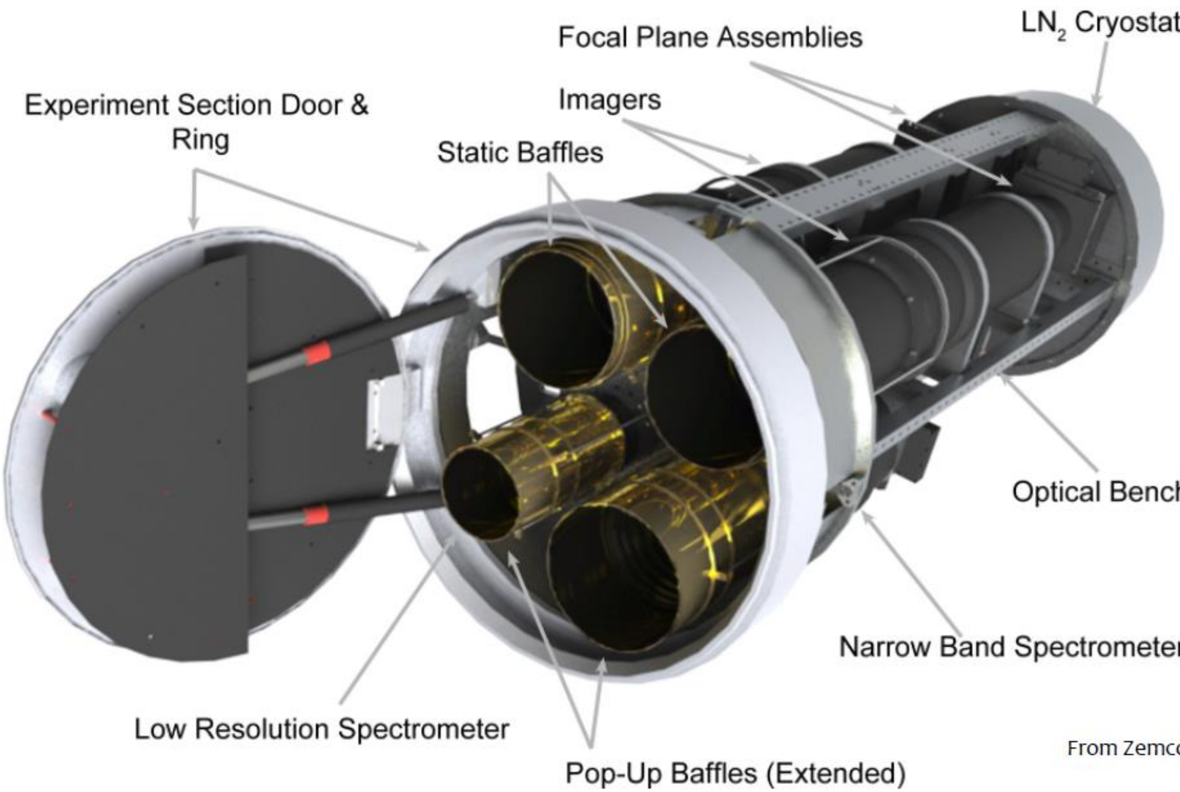

From Zemcov et al. (2012)

Axion Cosmophysics AIU2012, KEK, Nov 6-9, 2012

[From the slides of the talk by S Matsuura at AIU2012]

Launch vehicle & orbit

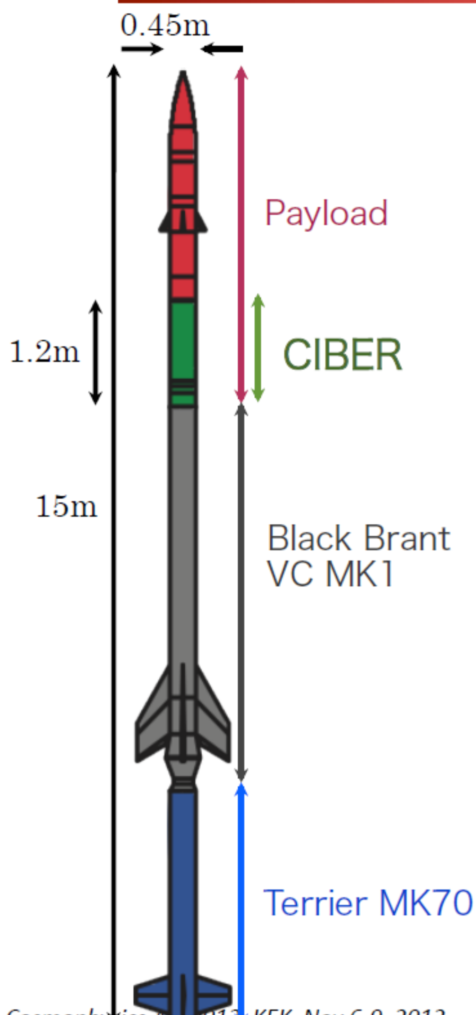

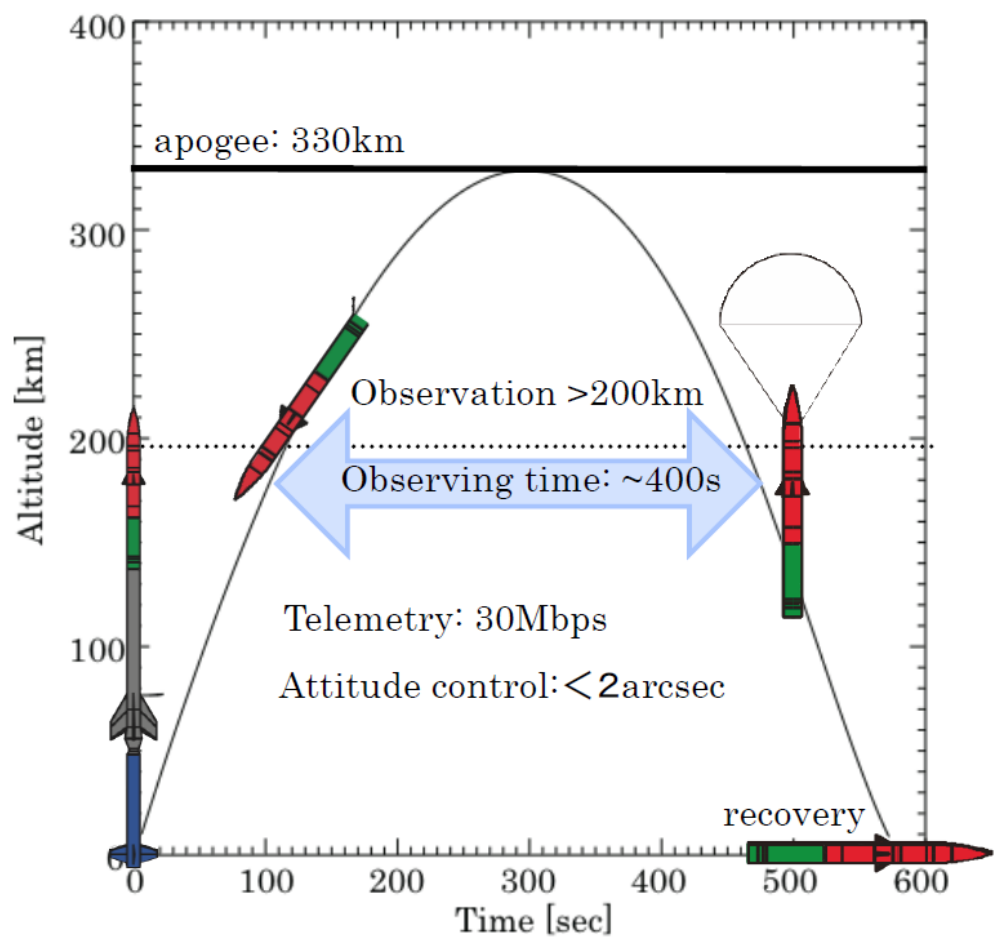

[From the slides of the talk by S Matsuura at AIU2012]

Rocket experiment CIBER

- We have already flown CIBER three times.
  (Feb 2009, Jul 2010 and Mar 2012)
- All flights were successful.
- Analyzing the data.

[From the slides of the talk by S Matsuura at AIU2012]

New measurements of CIRB by the rocket experiment CIBER

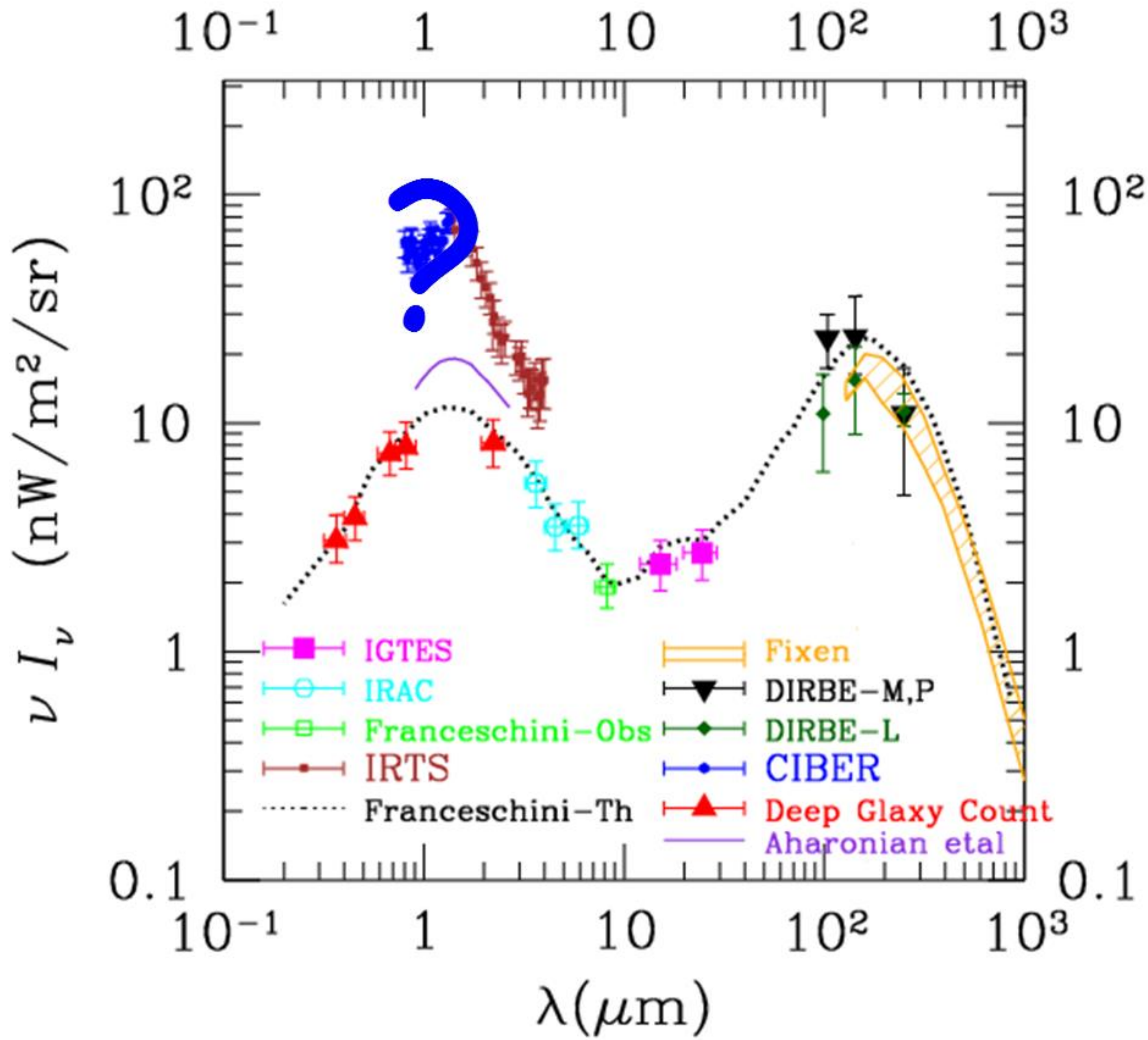

Making the Universe Transparent by Axions

Axion-Photon Conversion

- Chern-Simons coupling of axion with EM fields

$$\mathscr{L} = -\frac{1}{2}(\partial a)^2 - \frac{1}{2}m_a^2 a^2 - \frac{1}{2}F\cdot F - \frac{1}{2}g_{a\gamma} a F\cdot *F$$

$$\Downarrow$$

$$\mathscr{L} = \frac{1}{2}|\dot{a}|^2 - \frac{1}{2}\omega_a^2|a|^2 + \frac{1}{2}|\dot{\boldsymbol{A}}|^2 - \frac{1}{2}|\boldsymbol{k}\times\boldsymbol{A}|^2 - g_{a\gamma} a \boldsymbol{B}_0\cdot\dot{\boldsymbol{A}}$$

- Wave equations in plasma

$$\begin{aligned}
\epsilon\partial_t^2\boldsymbol{E} &= c^2\boldsymbol{k}\times(\mu^{-1}\boldsymbol{k}\times\boldsymbol{E}) - \frac{\omega_p^2\omega^2}{\omega^2-\omega_g^2}\boldsymbol{E} - g_{a\gamma}\omega^2 a\boldsymbol{B}_0 \\
&\quad + \frac{\omega_p^2}{\omega^2-\omega_g^2}\left\{i\omega\omega_g\boldsymbol{E}\times\boldsymbol{b} + \omega_g^2(\boldsymbol{E}\cdot\boldsymbol{b})\boldsymbol{b}\right\}, \\
\partial_t^2 a &= -\omega_a^2 a + g_{a\gamma}\boldsymbol{E}\cdot\boldsymbol{B}_0.
\end{aligned}$$

where

$$\omega_g = \frac{eB_0}{cm_e}, \quad \omega_p^2 = \frac{4\pi n_e e^2}{m_e}.$$

- High frequency limit

When a wave propagates nearly at the speed of light, we have

$$\partial_t X \approx -\partial_z X \approx -ikX$$

$$(\partial_t^2 - \partial_z^2)X(t,z) = (\partial_t - \partial_z)(\partial_t + \partial_z)X \simeq -2ik(\partial_t + \partial_z)X = -2ik\frac{dX}{dz}$$

Hence, the wave equations can be approximated by a first-order system of ODEs as

$$\left(-i\frac{d}{dz} - \mathscr{M}\right)\begin{pmatrix} A_\perp \\ A_{//} \\ a \end{pmatrix} = 0; \quad \mathscr{M} = \begin{pmatrix} \Delta_\perp & \Delta_R & 0 \\ \Delta_R & \Delta_{//} & \Delta_B \\ 0 & \Delta_B & \Delta_a \end{pmatrix}$$

where

$$\Delta_\perp = \Delta_{\rm pl} + \Delta_{\rm CM}^{\perp}, \quad \Delta_{//} = \Delta_{\rm pl} + \Delta_{\rm CM}^{//}, \quad \Delta_{\rm pl} = \omega_{\rm pl}^2/(2E)$$

$$\Delta_B = g_{a\gamma}B/2, \quad \Delta_a \simeq m_a^2/(2E)$$

Mass eigenvalues

Neglecting the Faraday rotation, the mass matrix can be diagonalised as

$$\begin{pmatrix} \Delta_\gamma & \Delta_B \\ \Delta_B & \Delta_a \end{pmatrix} = R(\theta)[\lambda_1, \lambda_2]R(-\theta) :$$

$$\lambda_1 + \lambda_2 = \Delta_\gamma + \Delta_a,$$
$$(\lambda_1 - \lambda_2)\cos(2\theta) = \Delta_\gamma - \Delta_a,$$
$$(\lambda_1 - \lambda_2)\sin(2\theta) = 2\Delta_B.$$

$$\Rightarrow \quad \lambda = \frac{1}{2}\{\Delta_\gamma + \Delta_a \pm \Delta_{\rm osc}\}; \quad \Delta_{\rm osc}^2 = (\Delta_\gamma - \Delta_a)^2 + 4\Delta_B^2$$

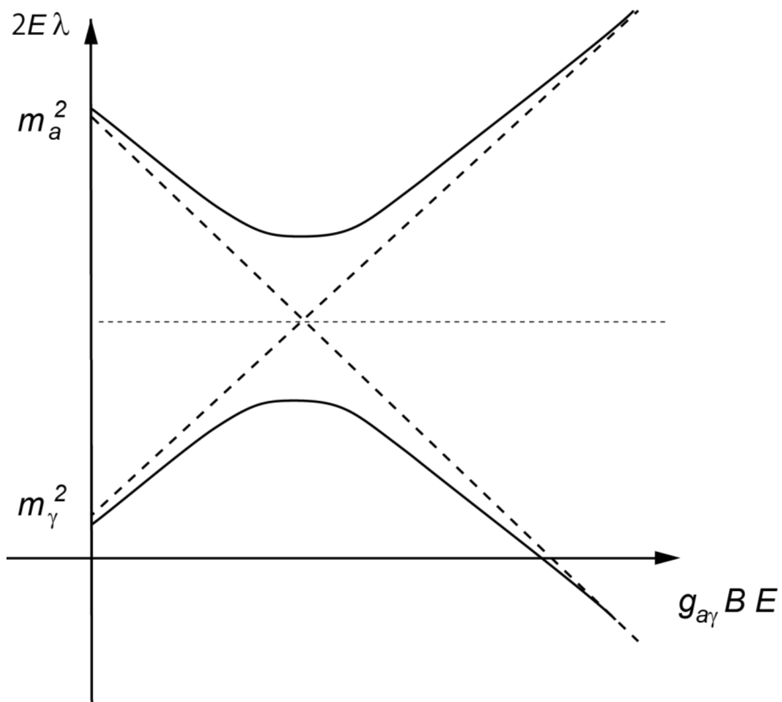

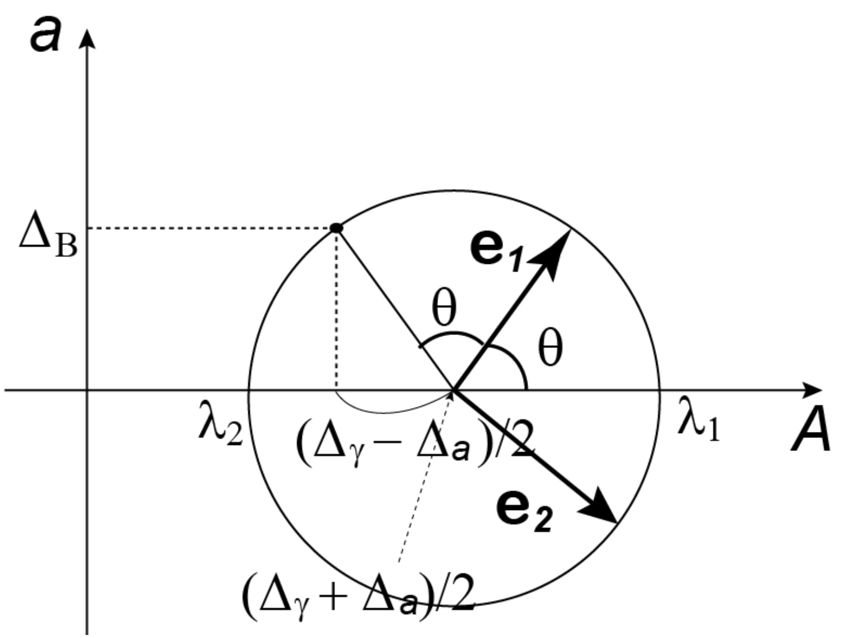

- Non-resonant transition

Neglecting the change of $\theta, \lambda_1, \lambda_2$, the solution is

$$\begin{pmatrix} A_{//}(z) \\ a(z) \end{pmatrix} = R(\theta) \begin{pmatrix} e^{i\lambda_1 z} & 0 \\ 0 & e^{i\lambda_2 z} \end{pmatrix} R(-\theta) \begin{pmatrix} A_{//}(0) \\ a(0) \end{pmatrix} .$$

Hence, the conversion rate is

$$P_{\gamma\to a} = P_0 := \sin^2(2\theta) \sin^2 \frac{s\,\Delta_{\rm osc}}{2} = \frac{4\Delta_B^2}{\Delta_{\rm osc}^2} \sin^2 \frac{s\,\Delta_{\rm osc}}{2}$$

where

$$\Delta_{\rm osc}^2 = (\Delta_{\rm CM} + \Delta_{\rm pl} - \Delta_a)^2 + 4\Delta_B^2.$$

- Resonant transition (non-uniform case)

$$2\pi|\Delta'_{\rm pl} + \Delta'_{\rm CM}| \lesssim \Delta_B^2 \Rightarrow \quad P_{\gamma\to a} = {\rm O}(1)$$

VHE gamma rays from AGNs can penetrate the CBR barrier

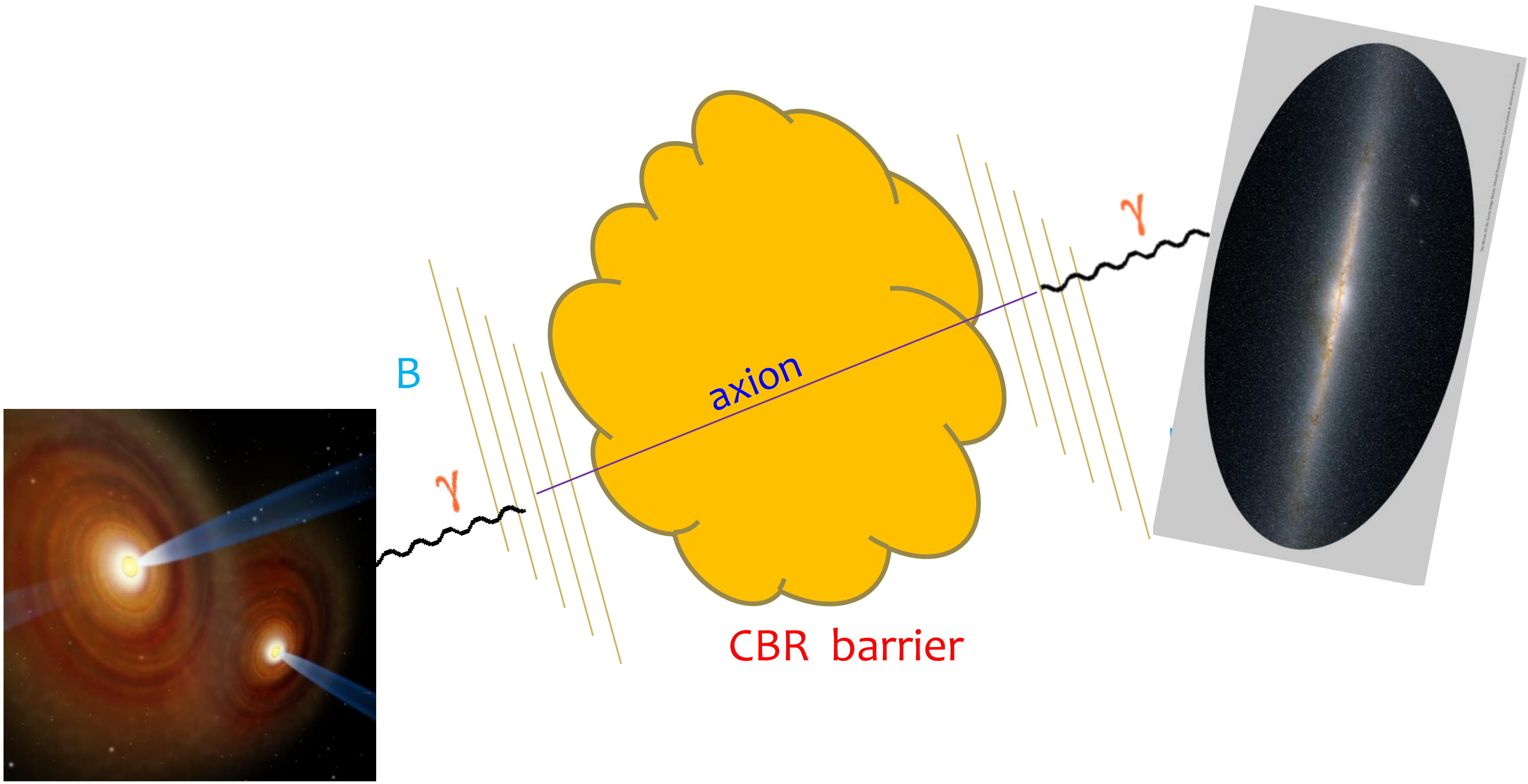

Conditions for Strong Conversion

- Conversion rate

$$P_0 = \frac{1}{1+(E_*/E)^2} \sin^2\left(g_{a\gamma} B \left[1+(E_*/E)^2\right]^{1/2} \frac{L}{2} \right),$$

$$E_* := \frac{|m_a^2 - m_\gamma^2|}{2 g_{a\gamma} B} \simeq 0.7 \frac{|m_a^2 - m_\gamma^2|}{(10^{-7}\mathrm{eV})^2} \left(\frac{10\mu\mathrm{G}}{B}\right) \left(\frac{g_{a\gamma}^{-1}}{10^{11}\mathrm{GeV}}\right) \mathrm{TeV}$$

- Condition 1: Near resonance

$$E \gtrsim E_* \Rightarrow \quad g_{a\gamma} \cdot 10^{11}\mathrm{GeV} \gtrsim 0.7 \left(\frac{m_a}{10^{-7}\mathrm{eV}}\right)^2 \frac{1}{B_{10\mu\mathrm{G}} E_{\mathrm{TeV}}}$$

- Consition 2: Sufficient oscillations

$$g_{a\gamma} B L \gtrsim \pi \Rightarrow \quad g_{a\gamma} \cdot 10^{11}\mathrm{GeV} \gtrsim 0.3 \frac{1}{B_{10\mu\mathrm{G}} L_{10\mathrm{kpc}}}$$

Axion solution

Kohri K, Kodama H, Ioka K: in preparation

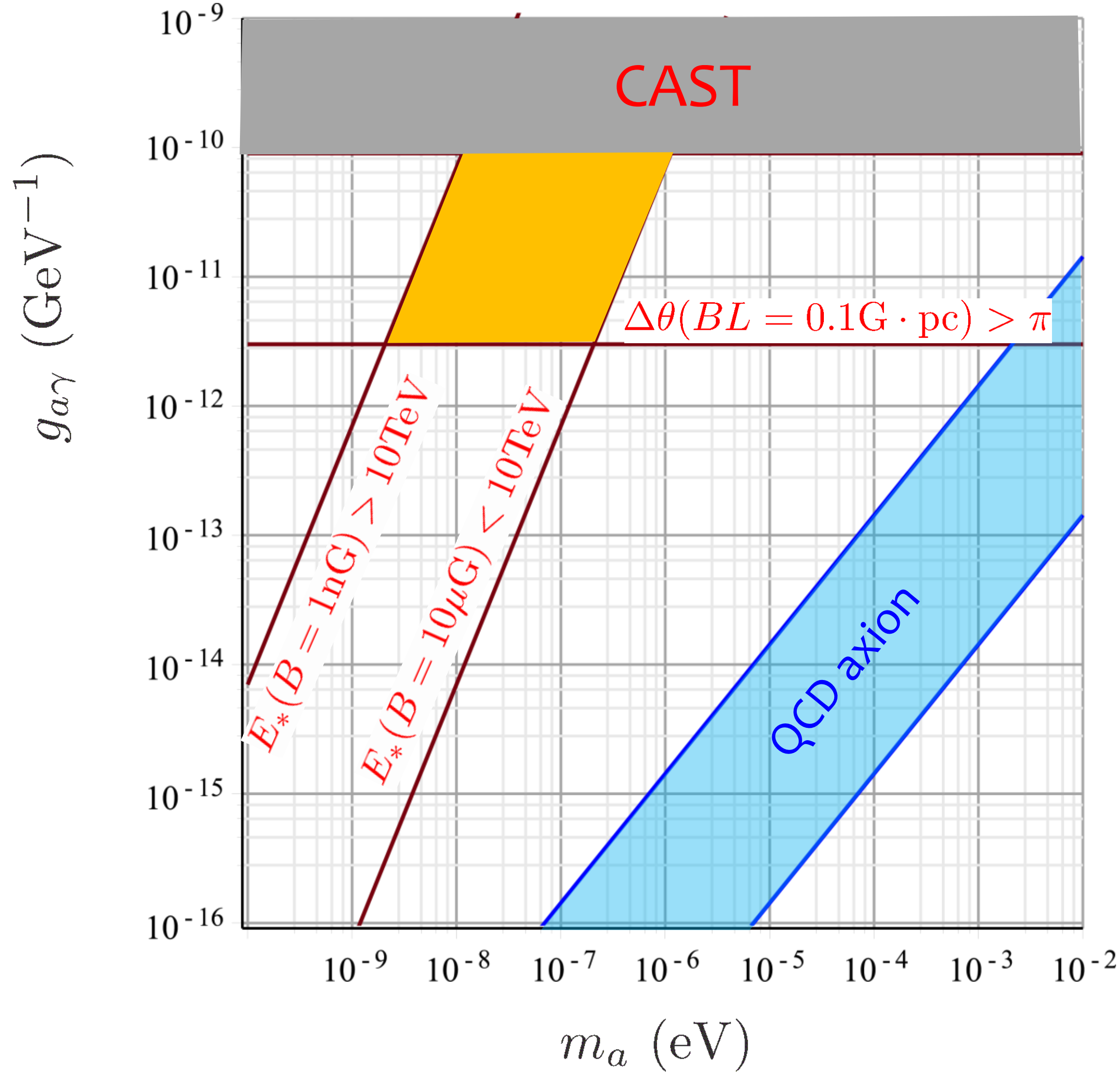

Summary

Summary

- Axionic Superradiance Instability

  - Superradiance instability produces recurrent phenomena of a linear growth of an axionic cloud around a rotating BH that is terminated and reset by bose nova collapse, if the axion mass m_a and the BH mass M satisfy the condition $GMm_a = O(1)$.

  - GW emissions from these phenomena can be detected by the ongoing and planned GW interferometers such as LIGO, KAGRA and the advanced LIGO, if they happen inside our galaxy.

  - Even null detection of GWs by these experiments can exclude axions with mass around 10^{-10} eV.

- Gamma Ray Astrophysics

  - Blazar observations by FERMI-LAT and IACTs are quite inconsistent with the flux of CIRB measured by CIBER.

  - In order to resolve this inconsistency by axion, its mass and coupling are strongly constrained: $m_a = 10^{-9} \sim 10^{-6}$ eV, $g_{a\gamma} = 10^{-11} \sim 10^{-10}$ GeV^{-1}